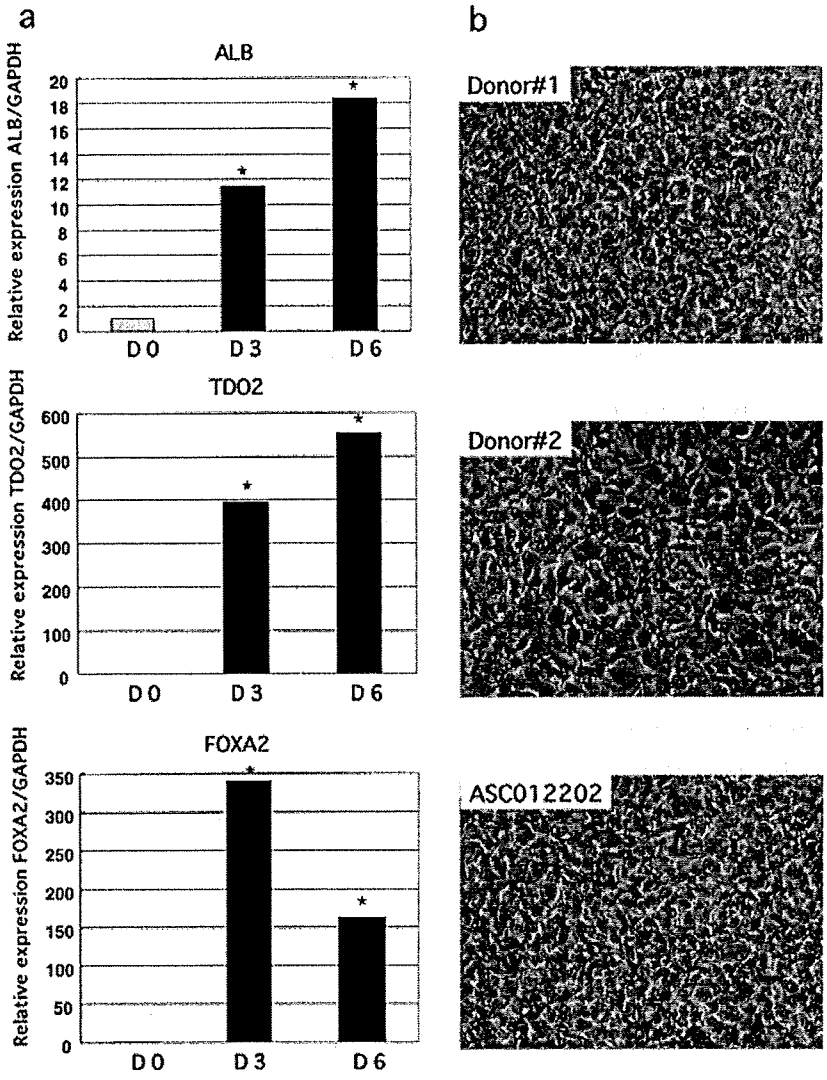

Figure 2 (a) Expression of albumin (ALB), tryptophan 2,3-dioxygenase (TDO2) and FOXA2 at day 3 (D3) (pretreatment with fibroblast growth factor [FGF]4 and Activin A) and day 6 (D6) (3 days of pretreatment with FGF4 and Activin A, and 3 days of treatment with hepatocyte growth factor [HGF], FGF1, FGF4, oncostatin M [OsM], dexamethasone [Dex], insulin-transferrin-selenium [ITS], dimethyl sulfoxide [DMSO], and nicotinamide) (■). Undifferentiated adipose-derived stem cells (ASC) (D0) (□). Data were analyzed by the Pair Wise Fixed Reallocation Randomization Test©, $n = 3$. $^*P < 0.05$). (b) Morphological features of ASC-derived hepatocyte-like cells of ASC derived from Donor #1, Donor #2, and commercially available ASC012202.

in Figure 3(a), changes in the morphology of ASC-derived hepatocyte-like cells (Donor #2) at days 0, 4, 9 and 16 of hepatogenic induction indicate hepatocyte maturation. At day 13, ASC-derived hepatocyte-like cells expressed albumin (Fig. 3b), which was detected by immunostaining, using anti-human specific antibody. Undifferentiated ASC, however, did not express albumin (data not shown). We also checked the functionality of ASC-derived hepatocyte-like cells. Figure 3(c) represents the albumin production at days 3, 6 and 9 of the induction process. ASC-derived hepatocyte-like cells also revealed an ability to uptake low-density lipoprotein (LDL) and store glycogen (Fig. 4).

Transplantation of ASC-derived hepatocyte-like cells into mice with liver injury

To address whether ASC reveal therapeutic abilities to regenerate an injured liver, we transplanted ASC-derived hepatocyte-like cells of Donors #1 and #2 into nude mice with acute liver failure. CCl_4 injury generated oxidative stress and hepatocyte necrosis. Twenty-four hours after CCl_4 injection, mice revealed serious liver injury. Biochemical parameters such as ALT, AST, UA and ammonia were increased in mice with CCl_4 injury compared with non-injured mice (Fig. 5). We transplanted 1.5×10^6 cells of ASC-derived hepatocyte-like cells into a CCl_4-injured mouse. After transplantation, ALT and AST were significantly decreased to a value more than 50% lower than in non-transplanted and injured mice (Fig. 5). Likewise, ammonia concentration was significantly decreased after ASC-derived hepatocyte-like cell transplantation. UA, a marker of oxidative stress, was significantly decreased up to a normal level after transplantation of ASC-derived hepatocyte-like cells (Fig. 5). Hematoxylin-eosin staining revealed that the level of injury was the same in the injured, non-transplanted mice (Fig. 6b,e) as well as in the injured transplanted mice (Fig. 6c,f), in contrast to the non-injured non-transplanted mice (Fig. 6a,d). Significant morphological changes between those mice, however, were detected in the hepatocytes of the non-necrotic area. The

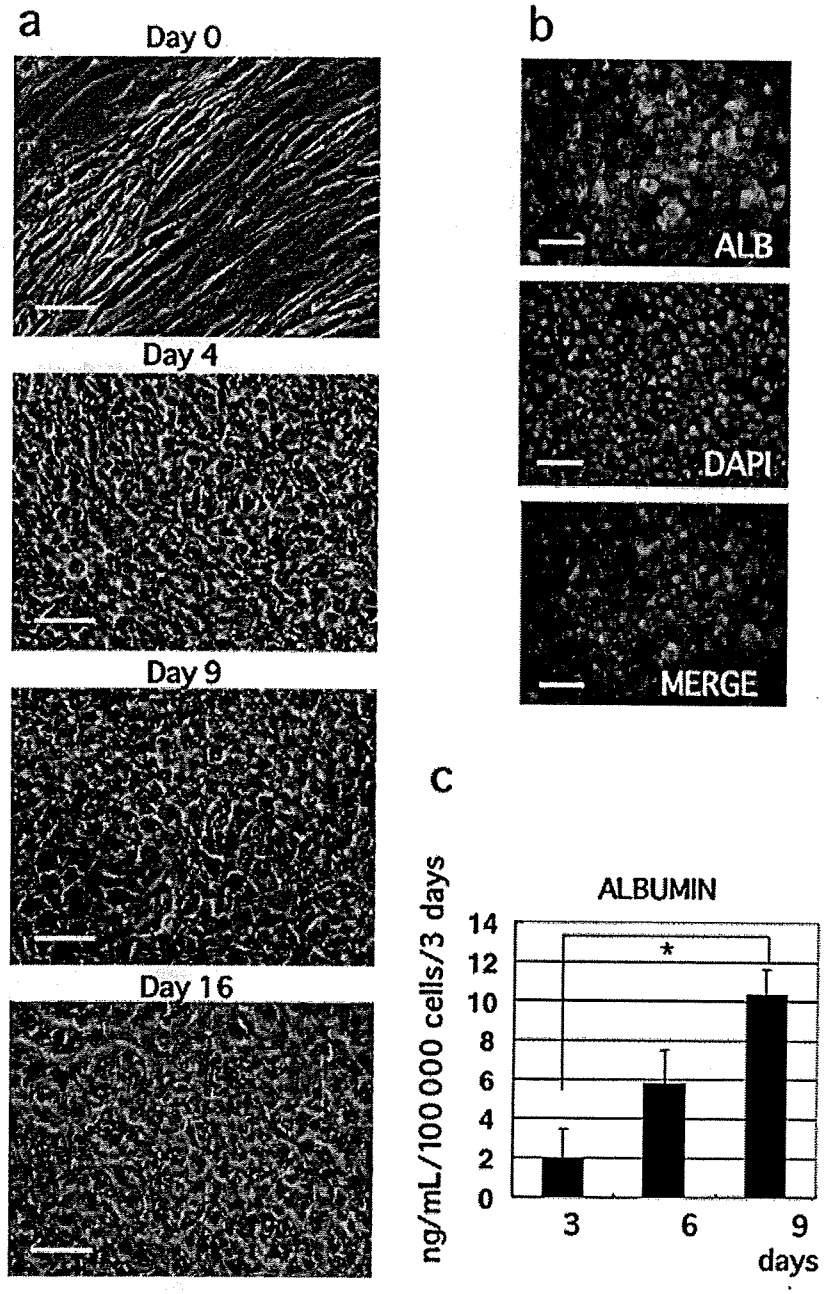

Figure 3 (a) Morphology of adipose-derived stem cells (ASC) (Donor #2) at days 0, 4, 9 and 16 during the hepatogenic induction process. (b) Albumin immunostaining analyses of ASC-derived hepatocyte-like cells at day 13 of induction. (c) Albumin production by ASC-derived hepatocyte-like cells at days 3, 6 and 9 of induction. Data are reported as the mean ± SD and were analyzed by Student's *t*-test, $n = 3$. $^*P < 0.05$). ALB, albumin; DAPI, 4,6-diamidino-2-phenylindole. Bar, 50 μm.

livers of injured, transplanted mice revealed less vacuolar degeneration caused by dilatation of mitochondria and rough endoplasmic reticulum. These observations reflect the data of the decrease of ALT and AST levels in injured transplanted mice. Therefore, transplantation of ASC-derived hepatocyte-like cells provided protection against CCl_4-induced hepatic injury. The above results indicate that ASC-derived hepatocyte-like cells generated within 13 days reveal hepatocyte-specific markers and functions *in vitro*, and improve liver function *in vivo*.

Discussion

Transplantation of hepatocytes generated from stem cells might become an easier, more efficient, and safer way than whole organ transplantation to cure patients suffering from liver disease. ASC can be very easily obtained with minimal invasiveness from a patient's own adipose tissue. Such a possibility sidesteps the obstacles regarding the risk of rejection, ethical issues, and availability of stem cells. We have already demonstrated mouse

Journal of Gastroenterology and Hepatology **24** (2009) 70–77

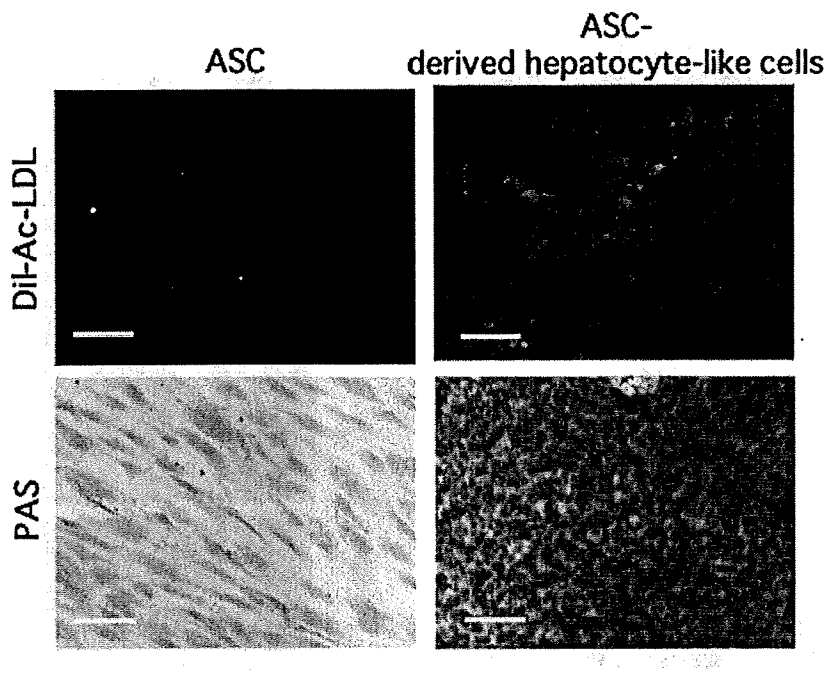

Figure 4 Low-density lipoprotein (LDL) uptake ability and glycogen storage ability (PAS) of adipose-derived stem cells (ASC)-derived hepatocyte-like cells at day 13 of induction. DiI-Ac-LDL, 1,1′-dioctade-cyl-3,3,3′,3′-tetramethyl-indocarbocyanine perchlorate (DiI)-labeled acetylated LDL. Bar, 50 μm.

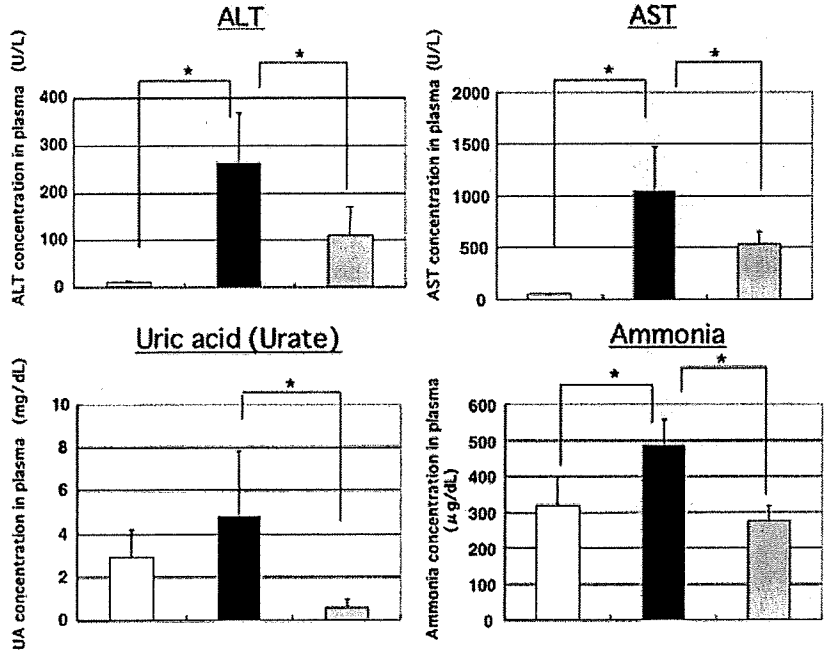

Figure 5 Biochemical analysis. Concentration of ammonia, alanine aminotransferase (ALT), aspartate aminotransferase (AST) and UA (uric acid/urate) in blood serum of killed mice. □, non-injured, non-transplanted mice; ■, injured and non-transplanted mice; ▨, injured and transplanted with adipose-derived stem cells (ASC)-derived hepatocyte-like cells (combined data of Donors #1 and #2). Data are presented as the mean ± SD and were analyzed by the Bonferroni correction $n = 3$. (* $P < 0.05$).

embryonic stem cell[28-30] and human adult ASC[19] hepatogenic differentiation.

In the present study, we presented induction within a very short time of human ASC into hepatocyte-like cells. Thirteen days is sufficient to generate *in vitro* cells, which reveal hepatocyte-specific morphology, marker profile, and functionality. This is first time for such a short hepatogenic differentiation protocol to be presented. At the beginning we treated the cells with Activin A together with FGF4, which are important factors at early stages of endoderm formation in mouse liver development. Afterwards we used a number of factors essential for hepatogenic specification and hepatocyte morphology maintenance. We compared the hepatocyte-like cells obtained by a new rapid protocol with the hepatocyte-like cells of an original protocol,[19] and have found that they reveal all the analyzed functions, albeit much earlier. We observed that 24 h of *in vitro* cocktail treatment (HGF, FGF1,

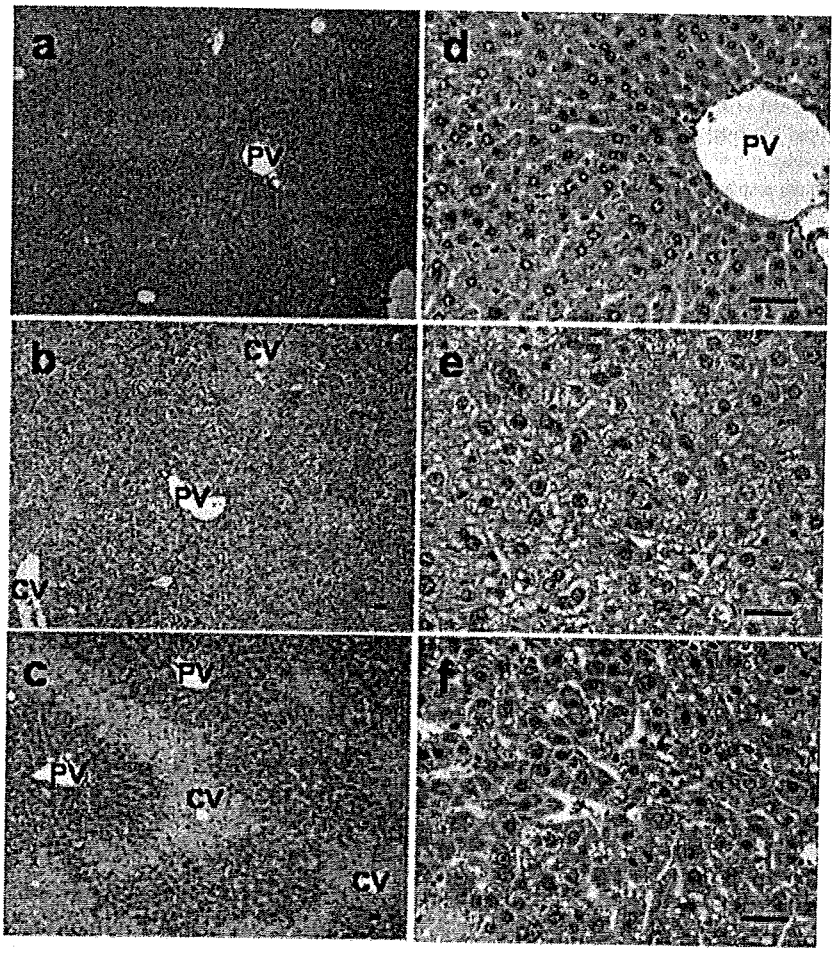

Figure 6 Hematoxylin-eosin staining of liver sections from (a,d) non-injured non-transplanted, (administered with olive oil and phosphate-buffered saline [PBS] [–]) mice ($n = 3$); (b,e) injured non-transplanted (administered with CCl_4 and PBS [–]) mice ($n = 3$); (c,f) injured transplanted (administered with CCl_4, 1 day after 1.5×10^6 ASC-derived hepatocyte-like cells transplantation) mice ($n = 4$). Panels a–c lower magnification 100 ×, panels d–f higher magnification 400 ×. CV, central vein; PV, portal vein. Scale bars represent 50 μm.

FGF4, OsM, Dex, ITS, nicotinamide, and DMSO) induces a dramatic change in morphology followed by little production of albumin at day 6 and a significant increase in the albumin level at day 9. However, using a previous protocol, albumin production was detected at days 30–50.

Prior to *in vivo* transplantation, it is important to induce hepatic fate within a short period of time and transplant the cells as fast as possible back into the patient with liver disease. Such a short period of time does not require large quantities of growth factors and may save much on expenses. Additionally, it will serve as hope and a great chance for a patient's total recovery. Significant morphological changes and albumin production as early as within 9 days suggest that it may be possible to even shorten the hepatic fate prior to transplantation. In the context of future clinical usage, a short period of stimulation to induce hepatic fate may be sufficient, because cells after transplantation may undergo further maturation in a regeneration environment.

Transplantation of *in vitro*-generated hepatocyte-like cells into CCl_4-injured nude mice resulted in the improvement of liver function *in vivo*. Interestingly, *in vivo* liver functions illustrated by the concentrations of ALT, AST, UA and ammonia were significantly decreased after ASC-derived hepatocyte-like cell transplantation (Fig. 5). The functional benefits of ASC-derived hepatocyte-like cell transplantation may be because of the functional support of the transplanted cells. It is still not clear by which mechanisms the transplanted cells improve the functioning of the liver. Fusion with host hepatocytes is not excluded. Likewise, the support and activation of endogenous progenitors are possible. Further studies examining the *in vivo* mechanism of homing, engraftment, and liver regeneration need to be conducted. It has been reported that in recipient liver, partial portal embolization, not partial portal ligation, improves engraftment of transplanted hepatocytes in a monkey primate preclinical model.[31] This provides new possibilities and strategies for future cell transplantation. It is essential to exclude any post-transplantation complications prior to any clinical trials. A long-term course experiment as well as safety issues should be carefully evaluated. Interestingly, in another study,[32] we observed that parameters such as ALT, AST, UA and ammonia were also decreased after undifferentiated ASC transplantation and we postulate that undifferentiated ASC per se compose a very attractive tool for the establishment of successful therapy for the liver.[32] We also speculate that the therapeutic potential of ASC may be due to the trophic activity of ASC.[32] These findings require additional studies with respect to safety issues post-

Journal of Gastroenterology and Hepatology **24** (2009) 70–77

transplantation; however, they give great promise for future clinical applications.

Short-term hepatogenic induction methods may also have great usage in drug metabolism studies and toxicological analyses. In fact, we have already observed that ASC-derived hepatocyte-like cells reveal cytochrome activities (data not shown).

In conclusion, our study revealed that ASC have a special affinity towards hepatocyte differentiation *in vitro* and hepatocyte regeneration *in vivo*. Thus, ASC may be a superior choice for the establishment of therapy for an injured liver.

Acknowledgments

This work was supported in part by a Grant-in-Aid for the Third-Term Comprehensive 10-Year Strategy for Cancer Control; Health Science Research Grants for Research on the Human Genome and Regenerative Medicine from the Ministry of Health, Labor, and Welfare of Japan; and a Grant from Japan Health Sciences Foundation. We would like to thank Dr Shinobu Ueda, Ms Ayako Inoue and Ms Maho Kodama from the National Cancer Center Research Institute for their valuable advice and assistance.

References

1 Thomas MB, Zhu AX. Hepatocellular carcinoma: the need for progress. *J. Clin. Oncol.* 2005; **23**: 2892–99.
2 Pittenger MF, Mackay AM, Beck SC *et al.* Multilineage potential of adult human mesenchymal stem cells. *Science* 1999; **284**: 143–7.
3 Bieback K, Kern S, Kluter H, Eichler H. Critical parameters for the isolation of mesenchymal stem cells from umbilical cord blood. *Stem Cells* 2004; **22**: 625–34.
4 De Coppi P, Bartsch G Jr, Siddiqui MM *et al.* Isolation of amniotic stem cell lines with potential for therapy. *Nat. Biotechnol.* 2006; **25**: 100–6.
5 Shih DT, Lee DC, Chen SC *et al.* Isolation and characterization of neurogenic mesenchymal stem cells in human scalp tissue. *Stem Cells* 2005; **7**: 1012–20.
6 In't Anker PS, Scherjon SA, Kleijburg-van der Keur C *et al.* Isolation of mesenchymal stem cells of fetal or maternal origin from human placenta. *Stem Cells* 2004; **22**: 1338–45.
7 Zuk PA, Zhu M, Mizuno H *et al.* Multilineage cells from human adipose tissue: implications for cell-based therapies. *Tissue Eng.* 2001; **7**: 211–28.
8 Zuk PA, Zhu M, Ashjian P *et al.* Human adipose tissue is a source of multipotent stem cells. *Mol. Biol. Cell* 2002; **13**: 4279–95.
9 Schwartz RE, Reyes M, Koodie L *et al.* Multipotent adult progenitor cells from bone marrow differentiate into functional hepatocyte-like cells. *J. Clin. Invest.* 2002; **109**: 1291–302.
10 Sato Y, Araki H, Kato J *et al.* Human mesenchymal stem cells xenografted directly to rat liver are differentiated into human hepatocytes without fusion. *Blood* 2005; **106**: 756–63.
11 Ong SY, Dai H, Leong KW. Inducing hepatic differentiation of human mesenchymal stem cells in pellet culture. *Biomaterials* 2006; **27**: 4087–97.
12 Lange C, Bruns H, Kluth D, Zander AR, Fiegel HC. Hepatocytic differentiation of mesenchymal stem cells in cocultures with fetal liver cells. *World J. Gastroenterol.* 2006; **12**: 2394–7.
13 Lee KD, Kuo TK, Whang-Peng J *et al.* In vitro differentiation of human mesenchymal stem cells. *Hepatology* 2004; **40**: 1275–84.
14 Snykers S, Vanhaecke T, Papeleu P *et al.* Sequential exposure to cytokines reflecting embryogenesis: the key for in vitro differentiation of adult bone marrow stem cells into functional hepatocyte-like cells. *Toxicol. Sci.* 2006; **94**: 330–41.
15 Kang XQ, Zang WJ, Bao LJ *et al.* Fibroblast growth factor-4 and hepatocyte growth factor induce differentiation of human umbilical cord blood-derived mesenchymal stem cells into hepatocytes. *World J. Gastroenterol.* 2005; **11**: 7461–5.
16 Hong SH, Gang EJ, Jeong JA *et al.* In vitro differentiation of human umbilical cord blood-derived mesenchymal stem cells into hepatocyte-like cells. *Biochem. Biophys. Res. Commun.* 2005; **330**: 1153–61.
17 Seo MJ, Suh SY, Bae YC, Jung JS. Differentiation of human adipose stromal cells into hepatic lineage in vitro and in vivo. *Biochem. Biophys. Res. Commun.* 2005; **328**: 258–64.
18 Talens-Visconti R, Bonora A, Jover R *et al.* Hepatogenic differentiation of human mesenchymal stem cells from adipose tissue in comparison with bone marrow mesenchymal stem cells. *World J. Gastroenterol.* 2006; **12**: 5834–45.
19 Banas A, Teratani T, Yamamoto Y *et al.* Adipose tissue-derived mesenchymal stem cells as a source of human hepatocytes. *Hepatology* 2007; **46**: 219–28.
20 Bartholomew A, Sturgeon C, Siatskas M *et al.* Mesenchymal stem cells suppress lymphocyte proliferation in vitro and in vivo and prolong skin graft survival in vivo. *Exp. Hematol.* 2002; **30**: 42–8.
21 Di Nicola M, Carlo-Stella C, Magni M *et al.* Human bone marrow stromal cells suppress T-lymphocyte proliferation induced by cellular or nonspecific mitogenic stimuli. *Blood* 2002; **99**: 3838–43.
22 Tse WT, Pendleton JD, Beyer WM, Egalka MC, Guinan EC. Suppression of allogeneic T-cell proliferation by human marrow stromal cells: implications in transplantation. *Transplantation* 2003; **75**: 389–97.
23 Lazarus HM, Haynesworth SE, Gerson SL, Rosenthal NS, Caplan AI. Ex vivo expansion and subsequent infusion of human bone marrow-derived stromal progenitor cells (mesenchymal progenitor cells): implications for therapeutic use. *Bone Marrow Transplant.* 1995; **16**: 557–64.
24 Le Blanc K, Tammik L, Sundberg B, Haynesworth SE, Ringden O. Mesenchymal stem cells inhibit and stimulate mixed lymphocyte cultures and mitogenic responses independently of the major histocompatibility complex. *Scand. J. Immunol.* 2003; **57**: 11–20.
25 McIntosh K, Zvonic S, Garrett S *et al.* The immunogenicity of human adipose-derived cells: temporal changes in vitro. *Stem Cells* 2006; **24**: 1246–53.
26 Arnalich-Montiel F, Pastor S, Blazquez-Martinez A *et al.* Adipose-derived stem cells are a source for cell therapy of the corneal stroma. *Stem Cells* 2008; **26**: 570–9.
27 Cui L, Yin S, Liu W *et al.* Expanded adipose-derived stem cells suppress mixed lymphocyte reaction by secretion of prostaglandin E2. *Tissue Eng.* 2007; **13**: 1185–95.
28 Teratani T, Yamamoto H, Aoyagi K *et al.* Direct hepatic fate specification from mouse embryonic stem cells. *Hepatology* 2005; **41**: 836–46.
29 Yamamoto Y, Teratani T, Yamamoto H *et al.* Recapitulation of in vivo gene expression during hepatic differentiation from embryonic stem cells. *Hepatology* 2005; **42**: 558–67.
30 Yamamoto H, Quinn Q, Asari A *et al.* Differentiation of embryonic stem cells into hepatocytes: biological functions and therapeutic application. *Hepatology* 2003; **37**: 983–93.
31 Dagher I, Boudechiche L, Branger J *et al.* Efficient hepatocyte engraftment in a nonhuman primate model after partial portal vein embolization. *Transplantation* 2006; **82**: 1067–73.
32 Banas A, Teratani T, Yamamoto Y *et al.* In vivo therapeutic potential of human adipose tissue-derived mesenchymal stem cells (ASCs), after transplantation into mice with liver injury. *Stem Cells* 2008; (in press).

Cytoplasmic tethering is involved in synergistic inhibition of p53 by Mdmx and Mdm2

Chihiro Ohtsubo,[1,3] Daisuke Shiokawa,[1,3,6] Masami Kodama,[1,3] Christian Gaiddon,[4] Hitoshi Nakagama,[2] Aart G. Jochemsen,[5] Yoichi Taya[1,3,6,7] and Koji Okamoto[1,2,3,7]

National Cancer Center Research Institute, [1]Radiobiology Division, [2]Early Oncogenesis Research Project, Tokyo, Japan; [3]SORST, Japan Science and Technology Corporation; [4]INSERM U692, Laboratoire de Signalisations Moleculaires et Neurode generescence, Universite de Strasbourg, Faculte de medecine, Strasbourg, France; [5]Department of Molecular and Cell Biology, Leiden University Medical Center, Leiden, The Netherlands

(Received February 17, 2009/Revised March 24, 2009/Accepted March 25, 2009/Online publication April 28, 2009)

The *mdm2* and *mdmx* oncogenes play essential yet nonredundant roles in synergistic inactivation of p53. However, the biochemical mechanism by which Mdmx synergizes with Mdm2 to inhibit p53 function remains obscure. Here we demonstrate that, using nonphosphorylatable mutants of Mdmx, the cooperative inhibition of p53 by Mdmx and Mdm2 was associated with cytoplasmic localization of p53, and with an increase of the interaction of Mdmx to p53 and Mdm2 in the cytoplasm. In addition, the Mdmx mutant cooperates with Mdm2 to induce ubiquitination of p53 at C-terminal lysine residues, and the integrity of the C-terminal lysines was partly required for the cooperative inhibition. The expression of subcellular localization mutants of Mdmx revealed that subcellular localization of Mdmx dictated p53 localization, and that cytoplasmic Mdmx tethered p53 in the cytoplasm and efficiently inhibited p53 activity. RNAi-mediated inhibition of Mdmx or introduction of the nuclear localization mutant of Mdmx reduced cytoplasmic retention of p53 in neuroblastoma cells, in which cytoplasmic sequestration of p53 is involved in its inactivation. Our data indicate that cytoplasmic tethering of p53 mediated by Mdmx contributes to p53 inactivation in some types of cancer cells. (*Cancer Sci* 2009; 100: 1291–1299)

The p53 tumor suppressor plays a central role in the prevention of tumorigenesis.[1,2] p53 exerts its function as a tumor suppressor by transcriptionally activating numerous target genes that are involved in inducing a variety of biological outcomes.[3–5] It is increasingly becoming evident that two related oncogenes, *mdm2* and *mdmx*, play central roles in the regulation of p53 activity.[6,7]

Analyses of knockout mice revealed that *mdmx* and *mdm2* suppress p53 in a nonredundant yet synergistic manner.[8] Mdmx and Mdm2 functionally cooperate to inhibit p53[9,10] and these inhibitors form a heterodimer complex through their RING finger domains.[11,12] Thus, Mdmx and Mdm2 play distinct yet cooperative functions for p53 inactivation, presumably via their physical interaction.

Mdm2 inactivates p53 by targeting it for ubiquitin-mediated proteasomal degradation and by promoting its transport from the nucleus into the cytoplasm,[13] and it is likely that inhibition of p53 by Mdm2 is attributed to these functions. Both functions of Mdm2 require the RING finger domain, which possesses E3 ubiquitin ligase activity. Indeed, Mdm2 functions as an E3 ubiquitin ligase for p53[14] although it has been reported that Mdm2 inhibits p53 via other mechanisms.[15]

In contrast to Mdm2, Mdmx lacks robust activity of an E3 ubiquitin ligase for p53[16] although Mdmx possesses a RING finger domain with high sequence similarity to that of Mdm2. In accordance with its inability to ubiquitinate p53 by itself, Mdmx-dependent inhibition of the transcriptional activity of p53 is independent of p53 degradation.[17] Recently, it was reported that Mdmx can complement the E3 activity of C-terminal mutants of Mdm2, suggesting that Mdmx contributes to p53 suppression in a manner distinct from Mdm2.[18,19]

In the present paper, by using nonphosphorylatable Mdmx mutants that are resistant to degradation by Mdm2, we showed that Mdmx and Mdm2 synergistically induce the cytoplasmic retention of p53 in DNA transfection assays. We demonstrated that cytoplasmic Mdmx, but not nuclear Mdmx, efficiently cooperates with Mdm2 to keep p53 in the cytoplasm and inhibits p53 activity. Further, RNAi-mediated inhibition of Mdmx or introduction of nuclear localization mutants of Mdmx reduced cytoplasmic retention of p53 in neuroblastoma cells. It has been documented that p53 is sequestered in the cytoplasm in some types of cancer, such as neuroblastoma, and the sequestration of p53 is likely to contribute to its inactivation. We will discuss how Mdmx and Mdm2 contribute to cytoplasmic sequestration of p53, and its implication during development of some types of cancer.

Materials and Methods

Cell lines. H1299 and U2OS cells were maintained in Dulbecco's modified Eagle's medium supplemented with 10% fetal calf serum.

Antibodies. Anti-Flag antibody (M2) was purchased from Sigma. Anti-p53 monoclonal antibody (DO-1) was purchased from Calbiochem. Anti-HA antibody was purchased from Roche (F Hoffmam-La Roche Ltd, Basel, Switzerland). Anti-myc-tag antibody (9E10), anti-GFP antibody (B-2), anti-topoisomerase I antibody (C-2), anti-γ tubulin antibody (D-10), and anti-Mdmx antibody (D-19) were purchased from Santa Cruz (Santa Cruz, CA).

DNA transfection. In DNA transfection experiments, 2 μg DNA and 4 μL Lipofectamine 2000 reagent (Invitrogen) were introduced per 2.0×10^5 cells. Transfected cells were then incubated for 20 h before harvesting. In experiments in which the subcellular localization mutants of Mdmx were transfected to determine localization of endogenous p53, Lipofectamine LTX (Invitrogen, Carlsbad, CA) was used instead according to the manufacturer's protocol.

Luciferase assay. Twenty hours after transfection, cells were lysed and luciferase activity was measured using the Dual-Luciferase Assay System (Promega, Madison, WI). Mean values (±SD) from three independent experiments were determined. Basal promoter activity expressed in the absence of HA-p53 was measured and subtracted in each experiment.

Immunostaining. Cells were fixed in 4% paraformaldehyde in PBS for 10 min, washed with 1× PBS, and permeabilized in 100% methanol for 30 min at −20°C. The fixed cells were then used for immunostaining as previously described.[20]

[6]Present address: Cancer Science Institute of Singapore, National University of Singapore, Singapore 117456.
[7]To whom correspondence should be addressed. E-mail: kojokamo@ncc.go.jp; nmiyt@nus.edu.sg

doi: 10.1111/j.1349-7006.2009.01180.x

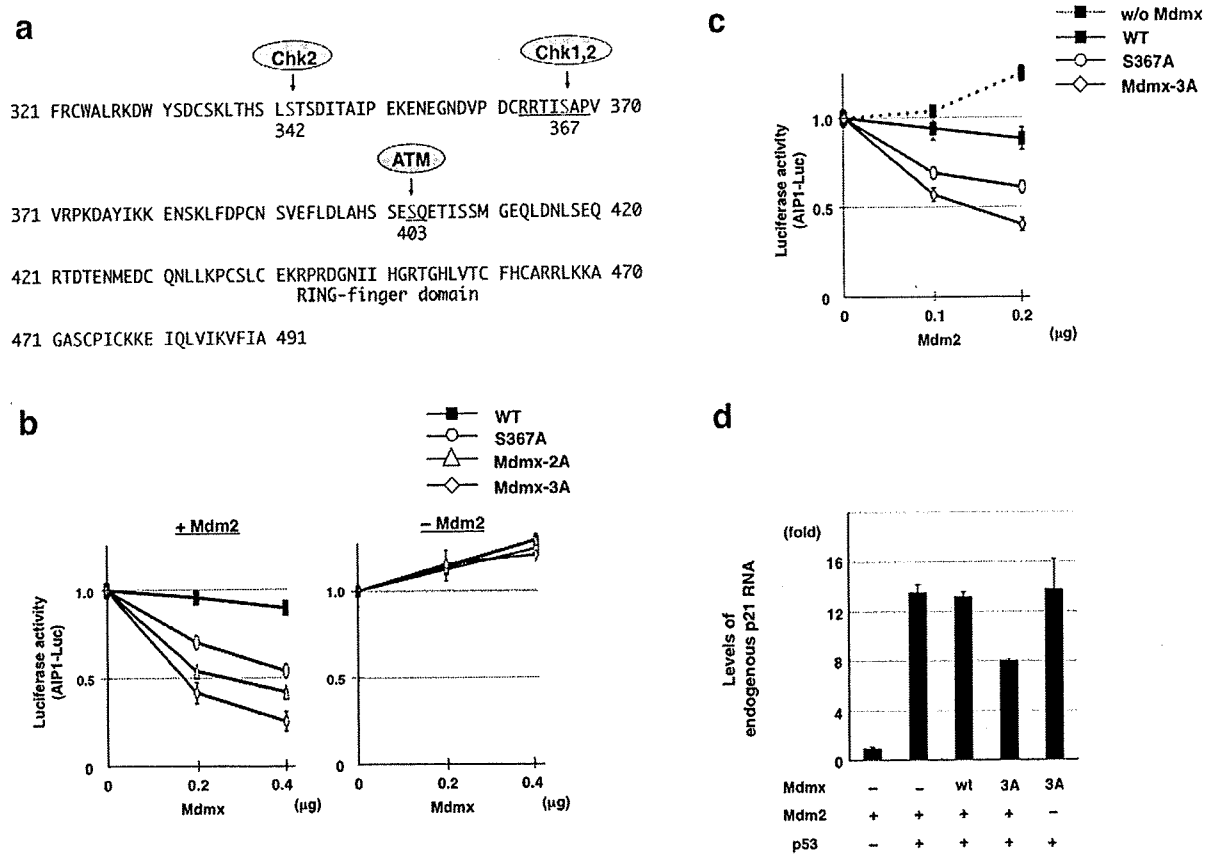

Fig. 1. Non-phosphorylatable Mdmx cooperates with Mdm2 to suppress p53. (a) Schematic representation of the positions of the Mdmx mutations. The serine residues phosphorylated after DNA damage are shown in red. The RING finger domain is shown in blue. (b,c) Inhibition of the transcriptional activity of p53 by the nonphosphorylatable mutants of Mdmx. (b) The indicated amounts of the wild-type Flag-Mdmx or Mdmx mutants were transfected into H1299 cells together with 0.15 μg HA-p53, 0.1 μg AIP-luc, and *Renilla* luciferase in the presence (left panel) or absence (right panel) of 0.2 μg myc-Mdm2. The total amount of transfected DNA was adjusted to 2 μg with pBluescript. Luciferase activity was measured 20 h after transfection. The numbers represent mean values ± standard deviations from experiments carried out in triplicate. The presented values were calculated as follows: value of cells transfected with the indicated amount of Mdmx/value of cells transfected without Mdmx. (c) The indicated amounts of myc-Mdm2 were transfected into H1299 cells together with 0.15 μg HA-p53, AIP-luc, *Renilla* luciferase, in the presence of 0.4 μg control vector, wild-type Flag-Mdmx, or the indicated Mdmx mutant. Luciferase assays were carried out as described in (b). (d) H1299 cells were cotransfected as described in (b). Total RNA prepared from transfected cells was used to measure the levels of endogenous p21 RNA by real-time RT-PCR using Taqman probe (Applied Biosciences, Foster City, CA). Levels of p21 were normalized with those of β-Actin.

shRNA infection. SH-SY5Y cells or IMR-32 cells were infected with lentiviruses as previously described.[21] Cells were infected with the control lentiviruses or the viruses that expressed the specific Mdmx shRNA overnight, incubated for an additional 2 days, and used for western blot analyses or immunostaining.

Additional information on Materials and Methods is provided in the Supporting Information.

Results

Non-phosphorylatable Mdmx effectively cooperates with Mdm2 to suppress p53 activity in H1299. Cellular stresses such as DNA damage cause degradation of Mdmx, via its phosphorylation by damage-induced kinases.[22] Serine 367 (S367) of Mdmx is phosphorylated after DNA damage, and alanine substitution of S367 (S367A), which mimics the nonphosphorylated form, promotes the cooperation between Mdmx and Mdm2 to inhibit p53 activity.[23] In addition to S367, two other serine residues comprise the major phosphorylation sites of Mdmx after DNA damage.[22] One of these sites, serine 403 (S403), is phosphorylated by ATM kinase,[22] whereas its downstream kinases, Chk1 or Chk2, phosphorylate serine 342 (S342) and S367, and facilitate the binding of 14-3-3 to Mdmx[22,24–26] (Fig. 1a). Phosphorylation of each site stimulates the proteasome-mediated degradation of Mdmx via its ubiquitination by Mdm2.[22,23,25]

Assuming that the phosphorylation of S342 and S403, in addition to S367, also compromises p53 suppression by Mdmx, we speculated that additional alanine substitution of S342 and S403 would allow Mdmx to inhibit p53 more effectively. We created the Mdmx mutants with the alanine substitution at S342 (Mdmx-2A) or at S342 plus S403 (Mdmx-3A) in addition to S367A, and introduced each mutant into p53-deficient H1299 cells together with p53 and the p53-responsive luciferase reporter (AIP-luc), in the presence or absence of the transfected Mdm2. Subsequently, the inhibitory effect of each Mdmx mutant on p53 activity was examined (Fig. 1b,c). Low amounts of Mdm2 were transfected so that introduction of Mdm2 alone did not inhibit p53 activity (Fig. 1c). As we reported previously,[23] the S367A mutation augmented the inhibition of p53 activity by Mdmx in the presence of transfected Mdm2 (Fig. 1b,c). The additional alanine substitution at S342 and S403 enhanced the ability of Mdmx to suppress p53 (Fig. 1b,c). In contrast, none of these mutants showed an inhibitory effect on p53 activity in the absence of the transfected Mdm2 (Fig. 1b). We observed similar Mdm2-dependent inhibition

doi: 10.1111/j.1349-7006.2009.01180.x

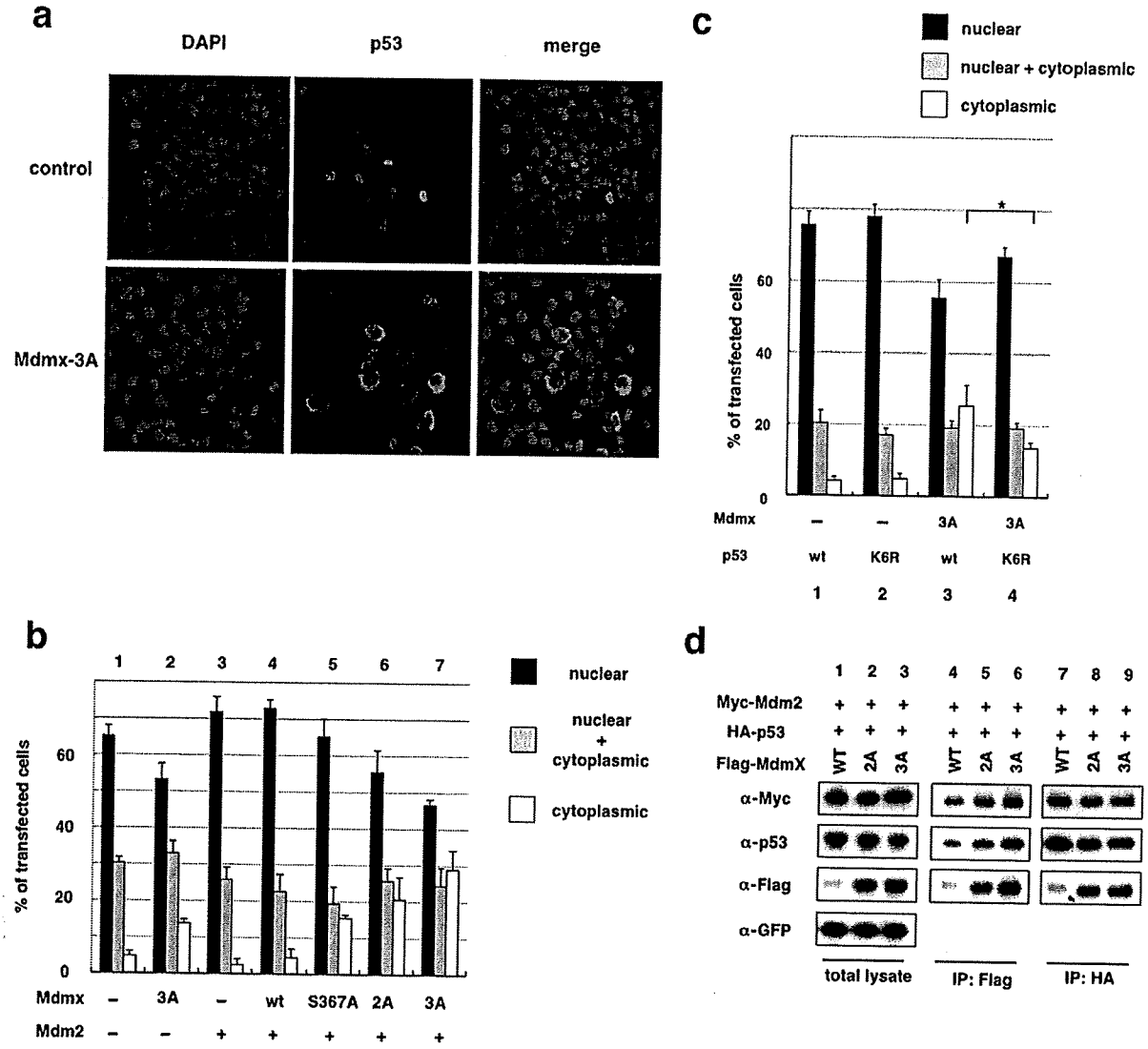

Fig. 2. Non-phosphorylatable Mdmx cooperates with Mdm2 to induce cytoplasmic localization of p53 in H1299. (a) H1299 cells were cotransfected with HA-p53 and myc-Mdm2, in the presence or absence of Mdmx-3A, and used for staining with DAPI and anti-HA antibody. Representative staining of the transfected cells is shown. (b) H1299 cells were cotransfected with the indicated Flag-Mdmx mutants and HA-p53 in the absence (columns 1 and 2) or presence (columns 3–7) of myc-Mdm2, and used for staining with anti-HA antibody. Subcellular localization of p53 of 100 transfected cells was evaluated in triplicate, and the average percentage of cells with the indicated staining pattern of p53 is shown. (c) Wild-type HA-p53 or HA-p53-K6R was transfected into H1299 cells together with myc-Mdm2 in the presence or absence of Flag-Mdmx-3A. Immunostaining analyses were carried out as described in (b). Asterisks indicate statistically significant differences ($P < 0.05$) as given by a one-way ANOVA followed by Tukey post-test. (d) HA-p53, myc-Mdm2, and GFP were transfected into H1299 together with the indicated Flag-tagged Mdmx as described in (b), and lysates prepared from transfected cells were used for immunoprecipitation (IP) with anti-Flag antibody (lanes 4–6) or anti-p53 (DO-1) antibody (lanes 7–9). The total lysates (lanes 1–3) and the immunoprecipitates were analysed by western blot analyses with the indicated antibodies.

of p53 activity by Mdmx-3A on another p53-responsive promoter (Bax-luc) (Supporting Information Fig. S1a). Wild-type Mdmx had an inhibitory effect that was comparable to that of Mdmx-3A in the presence of a chk2 inhibitor (Supporting Information Fig. S1b), suggesting that wild-type Mdmx is capable of inhibiting p53 in the absence of inhibitory phosphorylation.

Cotransfection of Mdm2 with these mutants suppressed the inhibitory effects of p53 on cell growth (Supporting Information Fig. S1c). In accordance with the inhibition of cell growth, Mdmx-3A, but not wild-type Mdmx, inhibits RNA expression of endogenous p21, which is a crucial target of p53 and inhibits cell cycle progression (Fig. 1d). Taken together, these data suggest that non-phosphorylated forms of Mdmx effectively cooperate with Mdm2 to inhibit p53 function.

Non-phosphorylatable Mdmx cooperates with Mdm2 to induce cytoplasmic localization of p53 in H1299. It has been demonstrated that low levels of Mdm2 inhibit p53 by inducing nuclear export.[27] In order to determine whether the nonphosphorylatable mutants of Mdmx cooperate with Mdm2 to inhibit p53 activity by stimulating cytoplasmic localization of p53, we next examined the subcellular localization of p53 after cotransfection of Mdmx, Mdm2, and p53 under the same conditions described in Figure 1(b). Introduction of Mdm2 alone did not significantly affect nuclear localization of p53 (Fig. 2a,b). Although cointroduction of Mdm2 and wild-type Mdmx had only a marginal effect on enhancement of cytoplasmic localization of p53 (Fig. 2b), cointroduction of Mdm2 and Mdmx-3A markedly enhanced a fraction of transfected cells with cytoplasmic p53 staining (Fig. 2a,b). Cytoplasmic

localization of p53 induced by Mdmx-3A alone was much less striking if compared to that induced by Mdm2 and Mdmx-3A (Fig. 2b), indicating that the effect of Mdmx-3A on the subcellular localization is largely dependent on the cointroduced Mdm2. Of note, there was a gradual enhancement of the cytoplasmic localization of p53 as Mdmx harbored an increasing number of alanine mutations at the phosphorylation sites (i.e. Mdmx-wt < S367A < 2A < 3A) (Fig. 2b), indicating that the extent of the stimulation of the cytoplasmic localization by the nonphosphorylatable mutations parallels their inhibitory effect on p53 activity (Fig. 1b). The cooperative effect of Mdmx-3A and Mdm2 to stimulate cytoplasmic localization of p53 was also observed in U2OS cells (Supporting Information Fig. S2a).

Cellular stresses such as DNA damage cause degradation of Mdmx via its phosphorylation by damage-induced kinases.[22,28] Mdmx was highly phosphorylated at S367 in transfected H1299[23] (K. Okamoto, unpublished data). In the presence of a chk2 inhibitor, wild-type Mdmx is capable of inducing cytoplasmic localization of p53 to an extent comparable to that of Mdmx-3A (Supporting Information Fig. S2b), indicating that in the absence of the inhibitory kinase, wild-type Mdmx is capable of inhibiting p53 activity (Supporting Information Fig. S1b) and inducing cytoplasmic localization of p53. These observations suggest that Mdmx phosphorylation may occur during the procedure of DNA transfection, and that the nonphosphorylatable Mdmx mutation facilitates clear observation of the cooperative effects of Mdmx and Mdm2 on p53 inhibition, by negating the inhibitory effects of Mdmx phosphorylation.

Mutation at the C-terminal lysines of p53 partially compromises the inhibitory effects of Mdmx-mediated enhancement of ubiquitination and inhibition of p53. It has been documented that Mdm2 ubiquitinates p53 at the six C-terminal lysines, the integrity of which are required for its nuclear export.[29,30] In addition to ubiquitination, some of these lysines are targeted for other types of modification, including neddylation, acetylation, and methylation.[31,32] Recent publications have indicated that Mdmx rescues the catalytic activity of Mdm2 mutants for ubiquitination and neddylation of p53 *in vivo*.[18,19,33] In order to determine whether Mdmx-3A enhances Mdm2-dependent p53 ubiquitination, we examined whether Mdmx enhances Mdm2-mediated ubiquitination in transfected H1299. Indeed, Mdmx-3A synergized with Mdm2 to induce p53 ubiquitination (Supporting Information Fig. S2c). In order to determine whether cooperative ubiquitination targets the C-terminal lysines of p53 by Mdmx and Mdm2, we created a mutant p53 in which all six lysines at the C-terminal domain were substituted with arginine (p53-K6R). *In vivo* ubiquitination assays confirmed that the K6R mutation eliminates the majority of p53 ubiquitination in transfected H1299 (data not shown). The K6R mutation partially inhibited Mdmx-3A-mediated cytoplasmic localization of p53 (Fig. 2c) and transcriptional inhibition of p53 (Supporting Information Fig. S2d). Thus, modification of the six lysines is partly required for Mdmx-dependent cytoplasmic localization and inactivation of p53, yet there exist other mechanisms by which Mdmx and Mdm2 cooperate to suppress p53 function.

Non-phosphorylatable mutations of Mdmx increase levels of the association of Mdmx to Mdm2 and p53. Next we determined whether the nonphosphorylatable mutations of Mdmx affect the levels of transfected p53, Mdm2, and Mdmx as well as the interaction among them (Fig. 2d). Mdmx-2A or Mdmx-3A expression did not markedly decrease the levels of p53 (Fig. 2d). In contrast, both the Mdmx-2A and Mdmx-3A mutations clearly increased the levels of introduced Mdmx (Fig. 2d). The levels of wild-type Mdmx and the Mdmx mutants were comparable in the presence of a proteasomal inhibitor MG132 (Supporting Information Fig. S2e), suggesting that the nonphosphorylatable mutations render Mdmx less sensitive to Mdm2-dependent proteasomal degradation.[22] In accordance with increased levels of Mdmx-2A and Mdmx-3A, the Mdmx mutations led to increased levels of the association of Mdmx to Mdm2 and p53 (Fig. 2d). These results indicate that the nonphosphorylatable mutations, by protecting Mdmx from Mdm2-dependent degradation, increase levels of the association of Mdmx to Mdm2 and p53.

Mdmx-3A mutation stimulates the association of Mdmx with Mdm2 and p53 predominantly in the cytoplasm. In order to examine whether the Mdmx-3A mutation affects subcellular localization of Mdmx and/or Mdm2 as well as p53, we next carried out immunostaining analyses of transfected Mdm2 and Mdmx. In agreement with a previous report,[10] transfected wild-type Mdmx was predominantly localized to the cytoplasm (Fig. 3a). Both wild-type Mdmx and Mdmx-3A mainly remained in the cytoplasm either in the presence or absence of cotransfected Mdm2 (Fig. 3a). Mdm2 predominantly localized to the nucleus in the absence of transfected Mdmx (Fig. 3b). Cotranfection of wild-type Mdmx mildly enhanced cytoplasmic localization of introduced Mdm2, and the extent of the cytoplasmic localization was markedly augmented by the Mdmx-3A mutation (Fig. 3b). Thus, the Mdmx-3A mutation facilitates cytoplasmic localization of cointroduced Mdm2.

The positive effects of Mdmx-3A mutation on the levels of the Mdmx–Mdm2 complex (Fig. 2d) and on the cytoplasmic localization of Mdm2 (Fig. 3b) suggest that the mutation leads to an increase of the Mdmx–Mdm2 complex in cytoplasm. Therefore, we next examined the extent of their interaction in each subcellular compartment after subcellular fractionation. In agreement with the results of the immunostaining (Fig. 3a,b), both Mdmx-3A and Mdm2 were mainly localized to the cytoplasm, and the Mdmx-3A–Mdm2 complex was predominantly formed in the cytoplasm (Fig. 3c). Cytoplasmic Mdmx-3A clearly colocalized with not only Mdm2 (data not shown) but also with p53 (Fig. 3d). Analyses of the subcellular localization of Mdmx-3A and p53 or of Mdmx-3A and Mdm2 in individual cells revealed that localization of Mdmx-3A in the cytoplasm was clearly associated with cytoplasmic localization of p53 (Supporting Information Fig. S3a) and Mdm2 (Supporting Information Fig. S3b). These data indicate that the Mdmx-3A mutation leads to an increase in the association of Mdmx with p53 and Mdm2 in the cytoplasm.

Cytoplasmic Mdmx is responsible for p53 localization in cytoplasm. In order to determine whether cytoplasmic Mdmx-3A induces localization of p53 to the cytoplasm, we generated Mdmx mutants in which either a peptide that corresponds to a nuclear localization signal of SV40 large T antigen (PKKKRKV) or a nuclear export signal of Rev of human immunodeficiency virus type-1 (LQLPPLERLTL) was connected to Mdmx-3A (NLS-Mdmx-3A or NES-Mdmx-3A). Subsequently, we introduced these Mdmx mutants together with Mdm2 and p53, and evaluated the effect of subcellular localization of Mdmx-3A on Mdm2 and p53. As expected, NLS-Mdmx-3A and NES-Mdmx-3A showed predominant localization to nuclei and cytoplasm respectively (Fig. 4a,b). Clear cytoplasmic localization of Mdm2 (Fig. 4c) and p53 (Fig. 4d) was induced by NES-Mdmx-3A, but not by NLS-Mdmx-3A. Inhibition of transcriptional activity of p53 by Mdmx-3A was enhanced by NES-Mdmx-3A and rather reduced by NLS-Mdmx-3A (Fig. 4e). Thus, cytoplasmic Mdmx-3A tethers p53 to the cytoplasm, whereas it effectively inhibits p53 activity in transfected H1299 cells.

Mdmx in the cytoplasm promotes cytoplasmic retention of endogenous p53. Next we examined whether subcellular localization of Mdmx-3A dictates localization of endogenous p53. Wild-type Mdmx, Mdmx-3A, NES-Mdmx-3A, or NLS-Mdmx-3A was introduced into U2OS cells, in which wild-type p53 is expressed predominantly in nuclei,[34] and we determined whether the mutants affect the subcellular localization of endogenous p53. The Mdmx-3A mutants were expressed at comparable levels (Fig. 4f). As we observed in H1299, NLS-Mdmx-3A and NES-Mdmx-3A predominantly localized to nuclei and cytoplasm respectively (data not shown). Introduction of wild-type Mdmx did not significantly affect nuclear localization of p53. In contrast, introduction of the

doi: 10.1111/j.1349-7006.2009.01180.x

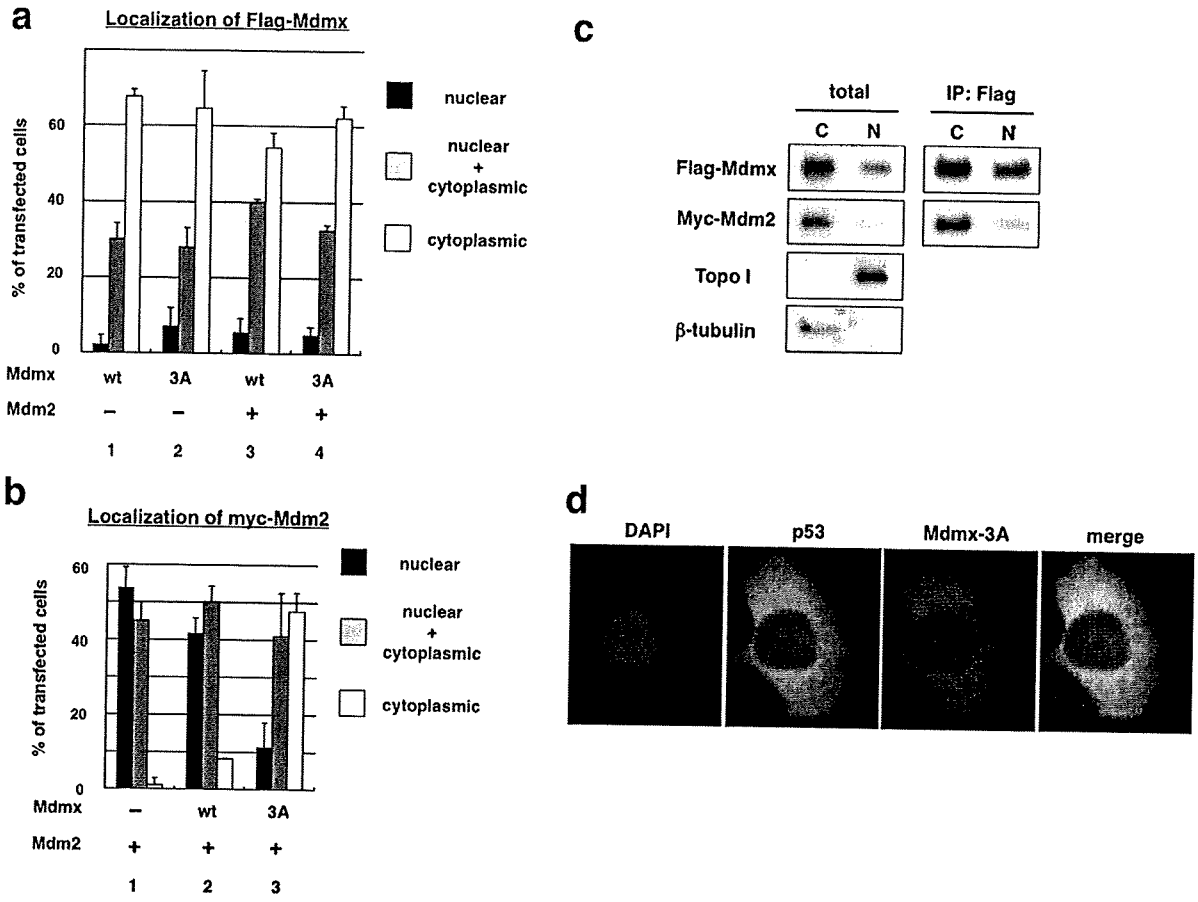

Fig. 3. The Mdmx-3A mutation stimulates the localization of Mdm2 and p53 predominantly to the cytoplasm. (a,b) HA-p53 was transfected into H1299 cells together with the indicated Flag-Mdmx in the presence or absence of myc-Mdm2 as described in Figure 2(b). The transfected cells were sequentially immunostained with (a) anti-Flag (M2) antibody or (b) antimyc antibody, antimouse IgG antibody conjugated with Alexa 595, and anti-HA antibody conjugated with Alexa 488 (Molecular Probe). Subcellular localization of (a) Flag-Mdmx or (b) myc-Mdm2 in cells that express HA-p53 was evaluated as described in Figure 2(b). (c) H1299 cells were transfected with HA-p53 together with Flag-Mdmx-3A and myc-Mdm2. The transfected cells were subjected to subcellular fractionation. The total lysates and the Flag-immunoprecipitates were then used for western blot analyses with the indicated antibodies. Topoisomerase I and γ tubulin are shown as nuclear and cytoplasmic markers respectively. (d) Representative staining of cells that express cytoplasmic p53 and Mdmx.

Mdmx-3A mutants induced localization of p53 to the cytoplasm, and a striking enhancement of cytoplasmic localization of p53 was observed in the presence of NES-Mdmx-3A (Fig. 4f). Taken together, these data indicate that cytoplasmically located Mdmx, presumably by tethering p53, induces localization of endogenous p53 to the cytoplasm.

Both Mdmx and Mdm2 predominantly localize to the cytoplasm of neuroblastoma cells. Inactivation of p53 via its cytoplasmic localization is frequently observed in some types of cancer such as neuroblastoma,[35] and yet the precise mechanism by which p53 is sequestered in cytoplasm remains obscure. It was reported that Mdm2 mediates the cytoplasmic retention of p53 in neuroblastoma.[36,37] In order to examine whether Mdmx as well as Mdm2 is involved in p53 inactivation via cytoplasmic sequestration in neuroblastoma, we analyzed SH-SY5Y and IMR-32 cells that, like most other neuroblastoma cells, harbor wild-type p53 with cytoplasmic localization (Fig. 5a; Supporting Information Fig. S4a). Expression levels of Mdmx in SH-SY5Y were much higher than those in normal human fibroblasts, and even higher than those in MCF-7 (data not shown), breast cancer cells in which the *mdmx* gene is amplified and Mdmx is expressed at high levels.[38] Both Mdmx and Mdm2 predominantly localized to the cytoplasm in SH-SY5Y cells (Supporting Information Fig. S4a). The extent of S367 phosphorylation in SH-5YSY cells was much lower than that in the transfected H1299 cells (Supporting Information Fig. S4c). These observations suggest that Mdmx is expressed, probably in nonphosphorylated forms, at high levels in the cytoplasm in unstressed SH-SY5Y cells.

Nuclear Mdmx inhibits cytoplasmic retention of p53 in SH-SY5Y. In order to determine whether subcellular localization of Mdmx-3A dictates localization of endogenous p53 in neuroblastoma cells as well as in U2OS cells, the effects of subcellular localization of wild-type Mdmx or the Mdmx mutants on endogenous p53 localization were evaluated as described in Figure 4(f). The Mdmx-3A mutants were expressed at comparable levels (Fig. 5b). In accordance with cytoplasmic localization of endogenous Mdmx (Supporting Information Fig. S4a), Mdmx-3A and wild-type Mdmx exclusively localized to the cytoplasm (Fig. 5b). As expected, the majority of NLS-Mdmx-3A localized to nuclei (87%) and NES-Mdmx-3A totally localized to the cytoplasm. Immunostaining of transfected SH-SY5Y cells revealed that the expression of NLS-Mdmx-3A, but not NES-Mdmx-3A, reduced cytoplasmic localization of p53 (Fig. 5b), indicating that nuclear expression of Mdmx-3A inhibits cytoplasmic retention of p53 in SH-SY5Y.

Mdmx is required for inactivation of p53 in neuroblastoma cells. In order to further examine the role of Mdmx in p53 inactivation

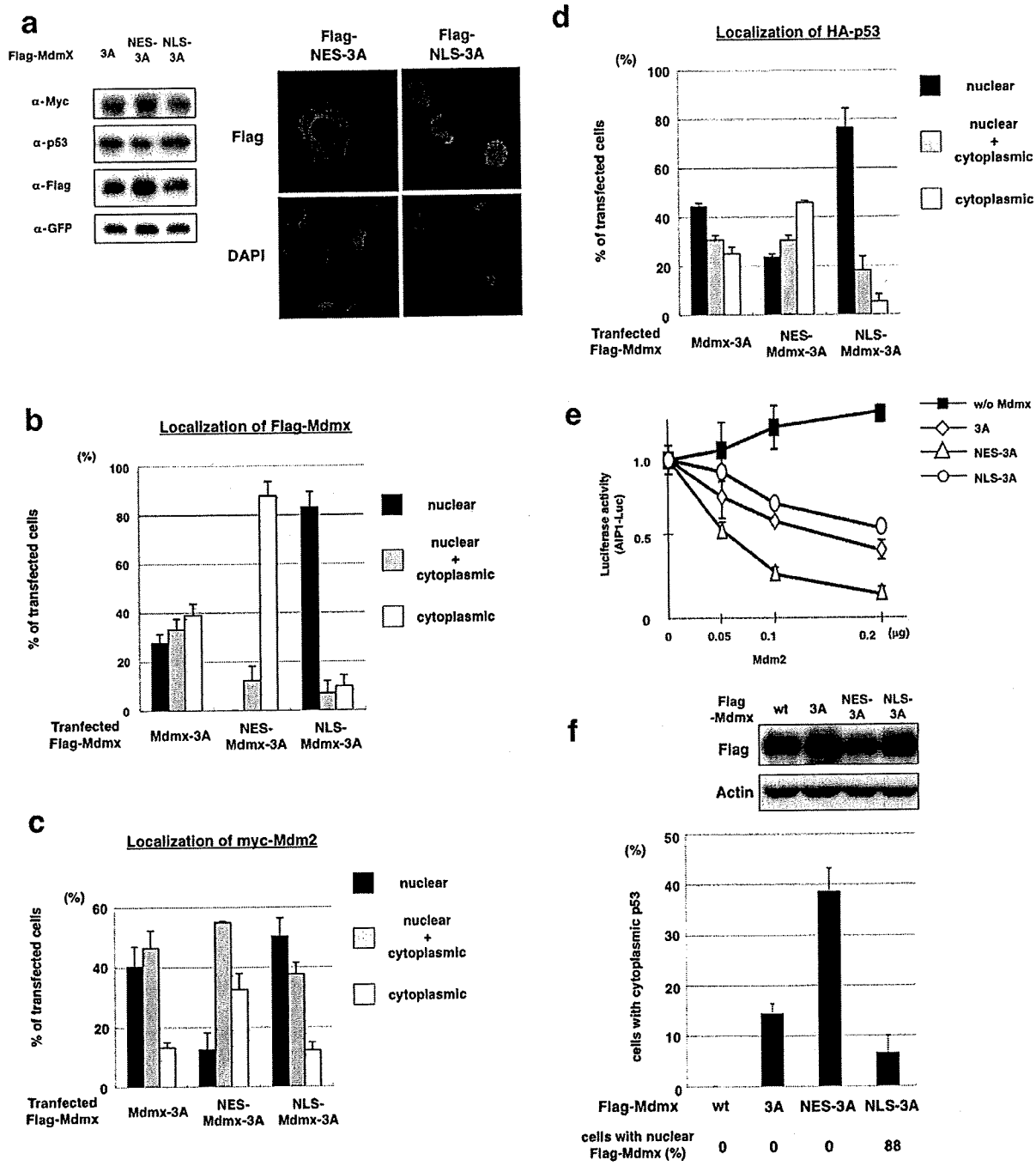

Fig. 4. Cytoplasmic Mdmx tethers p53 and Mdm2 to the cytoplasm and stimulates p53 inhibition. (a) H1299 cells were cotransfected with HA-p53, myc-Mdm2, GFP, and the indicated Flag-tagged Mdmx. Left panel, western blot analyses with the indicated antibodies. Right panel, representative staining with anti-Flag antibody and DAPI. (b–d) H1299 cells were transfected with the indicated Mdmx, together with myc-Mdm2, and immunostained with (b) anti-Flag antibody, (c) anti-Mdm2 antibody, or (d) anti-HA antibody. Subcellular localization of transfected (b) Mdmx, (c) Mdm2, or (d) p53 was represented as described in Figure 2(b). (e) Flag-Mdmx mutant or the control vector was transfected into H1299 cells together with HA-p53, in the presence of the indicated amounts of myc-Mdm2, and luciferase assays were carried out as described in Figure 1(c). (f) U2OS cells were transfected with the indicated Flag-Mdmx. Upper panel, western blot analyses with the anti-Flag or the anti-actin antibodies. Lower panel, cells transfected with the indicated plasmids were immunostained with the anti-Flag and antip53 (CM1) antibodies, and a fraction of the transfected cells with cytoplasmic p53 staining was quantified.

in neuroblastoma cells, we inhibited Mdmx expression by infecting cells with the lentiviruses expressing Mdmx shRNA. Mdmx inhibition by the specific shRNA, while not significantly affecting levels of p53, induced expression of p21, a crucial p53 target (Fig. 5c) and reduced the cytoplasmic localization of p53 (Fig. 5d,e). The positive role of Mdmx in cytoplasmic localization of p53 was confirmed by western blot analyses of nuclear and cytoplasmic lysates prepared from the infected cells. Depletion of Mdmx

doi: 10.1111/j.1349-7006.2009.01180.x

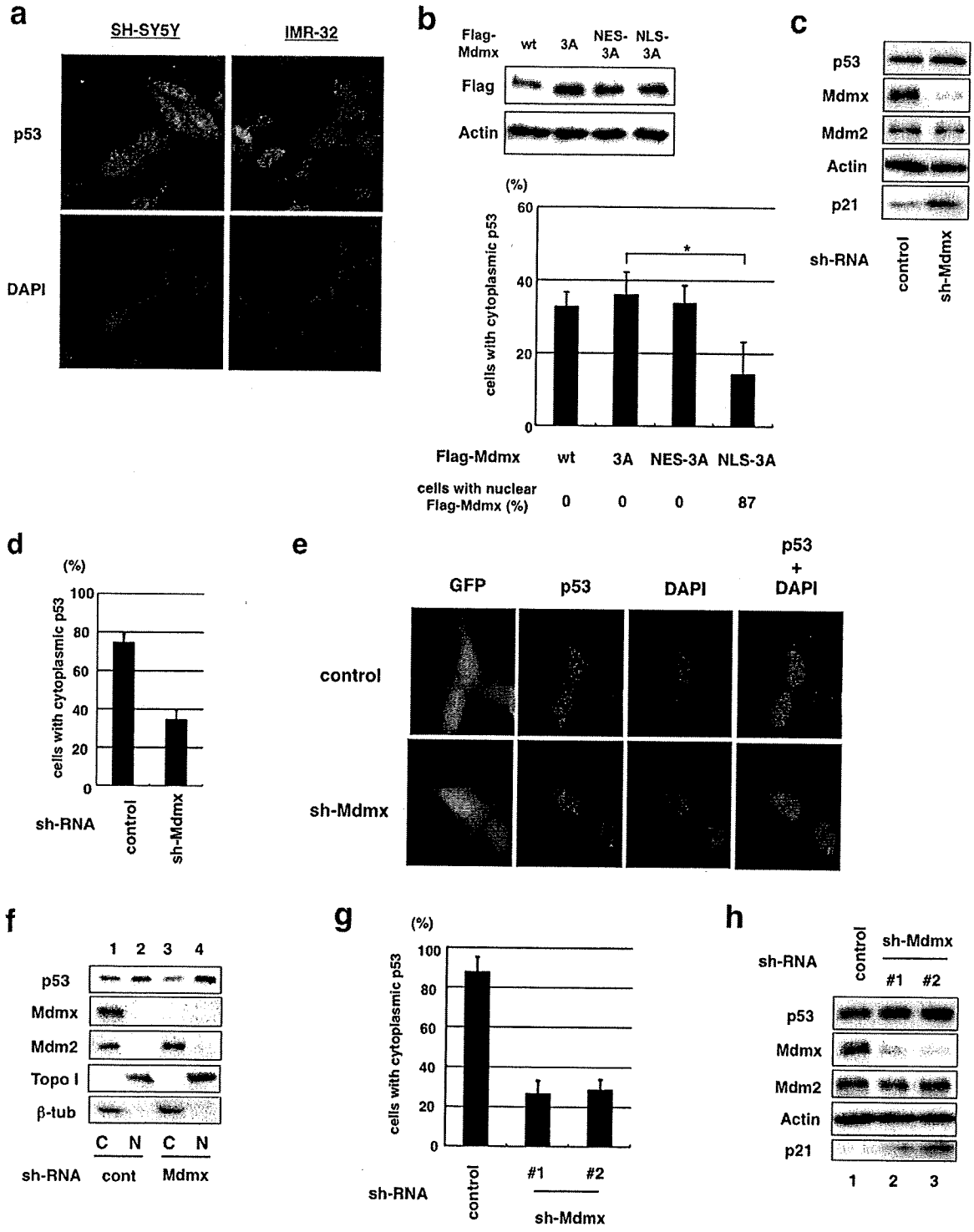

Fig. 5. Mdmx is required for cytoplasmic retention of p53 in neuroblastoma cells. (a) Cytoplasmic retention of p53 in neuroblastoma. SH-SY5Y or IMR-32 cells were stained with antip53 antibody (CM1) and DAPI. (b) SH-SY5Y cells were transfected with the indicated Flag-tagged Mdmx. Western blot analyses and quantification of a fraction of cells with cytoplasmic p53 were carried out as described in Figure 4(f). (c–f) SH-SY5Y cells were infected with the control lentivirus or the viruses expressing Mdmx shRNA. (c) Lysates prepared from the infected cells were used for western blot analyses with the indicated antibodies. (d) The infected cells were immunostained with antip53 polyclonal antibody (CM1) and DAPI. The average percentage of the infected cells with cytoplasmic staining of p53 was presented after evaluating subcellular localization of p53 of 100 cells in triplicate. (e) Representative pictures of staining of cells that were infected with the control lentiviruses or the viruses that express Mdmx shRNA. Note that the viruses express GFP, and infection efficiency is ~100% judging from GFP expression. (f) Subcellular fractionation and western blot analyses were carried out with the indicated antibodies. (g,h) IMR-32 cells were infected with the control lentiviruses or the viruses that express Mdmx shRNA, and (g) western blot analyses or (h) the quantification of subcellular distribution of p53 was carried out as described in (c) and (d) respectively.

decreased p53 levels in the cytoplasm and increased those in nuclei, while the depletion did not significantly affect cytoplasmic localization of Mdm2 (Fig. 5f).

Similarly, inhibition of Mdmx by the specific shRNA led to induction of p21 expression and inhibition of cytoplasmic localization of p53 in IMR-32, another neuroblastoma cell line (Fig. 5g,h; Supporting Information Fig. S4c). Thus, Mdmx contributes to cytoplasmic retention of p53 in neuroblastoma cells.

Discussion

Genetic evidence indicates that *mdmx* is a crucial inhibitor of p53 and that *mdmx* and *mdm2* cooperatively function to inhibit p53. However, the mechanical basis of the cooperation of the oncogenes is not clearly established. In an attempt to recapitulate synergistic inhibition of p53 by Mdmx and Mdm2, we took advantage of our observation that the nonphosphorylatable mutations confer Mdmx resistance against Mdm2-mediated degradation. We demonstrated that nonphosphorylatable mutations of Mdmx markedly enhance the ability of Mdmx to cooperate with Mdm2 for inhibition of p53, suggesting that the stress-induced phosphorylation of Mdmx is important for its ability to suppress p53. The importance of the Mdmx phosphorylation was further supported by the functionality of wild-type Mdmx on p53 suppression in the presence of a chk2 inhibitor (Supporting Information Figs S1b and 2b).

Through the analyses of the function of the Mdmx mutants, we found that the nonphosphorylatable mutant of Mdmx effectively cooperates with Mdm2 to induce p53 ubiquitination. The ability of the nonphosphorylatable mutations of Mdmx to inhibit p53 activity was associated with enhanced cytoplasmic retention of p53 and with increased levels of the interaction of Mdmx to p53 and Mdm2 in cytoplasm. A causal role of cytoplasmic Mdmx to induce localization of p53 in the cytoplasm was demonstrated using the Mdmx mutants that harbor autonomous subcellular localization signals.

p53 is sequestered in the cytoplasm in some types of cancer, and it is assumed that the sequestration of p53 contributes to p53 inactivation.[35,39] Mdm2 is essential for inhibition and cytoplasmic sequestration of p53 in neuroblastoma cells,[36,37] and the cooperative function of Mdmx and Mdm2 to induce p53 retention in the cytoplasm may contribute to its inactivation in some of cancer cells. We found that, in addition to Mdm2, Mdmx is also required for cytoplasmic sequestration of p53 in neuroblastoma cells. Considering that Mdm2 enhances the interaction between p53 and Mdmx in the transfected H1299 cells, Mdmx and Mdm2 may cooperate by stimulating the formation of a complex with p53. Of note, Mdmx stabilizes p53 via a formation of a complex with Mdm2,[16] and formation of such a stable complex may account for cytoplasmic sequestration of p53.

In addition to the cytoplasmic tethering via physical interaction, regulation of post-translational modification of the C-terminal of p53 is likely to contribute to the cooperative inhibition of p53 by Mdm2 and Mdmx, because mutations in the six C-terminal lysines, which are targets for the regulatory modification, partly abolished the cooperative inhibition of p53 (Supporting Information Fig. S2d). Mdm2 promotes cytoplasmic translocation of p53 via its ubiquitination at the same lysine residues,[27,40] and accumulating data[9,18,19] as well as ours (Supporting Information Fig. 2c) indicate that Mdmx promotes Mdm2-dependent p53 ubiquitination. Hence, it is likely that enhancement of Mdm2-dependent ubiquitination of p53 by Mdmx also contributes to the cooperative inhibition of p53 activity by these oncoproteins. In fact, the cytoplasmic retention of p53 in neuroblastoma is in part attributed to multimono-ubiquitination of p53 due to defective function of HAUSP, a de-ubiquitinating enzyme for p53 and Mdmx and Mdm2.[34,41,42] However, we did not observe a significant change in the pattern of p53 laddering, which presumably represents ubiquitinated p53, in neuroblastoma cells after knock down of Mdmx (data not shown). The two mechanisms that mediate cytoplasmic localization of p53, namely cytoplasmic tethering and ubiquitin-dependent translocation, are not mutually exclusive, and presumably contribute to cytoplasmic retention of p53 by Mdmx.

Acknowledgments

We are indebted to Jiandong Chen and Hirofumi Arakawa for providing us with Flag-Mdm2 and AIP-luc respectively. We thank Kenji Kashima for experimental assistance. This work was supported by a Grant-in-Aid for Scientific Research from the Ministry of Education, Culture, Sports, Science, and Technology of Japan (Y.T. and K.O.), a Grant-in-Aid for Third Term Comprehensive Control Research for Cancer from the Ministry of Health, Labor, and Welfare, Japan (Y.T.), the Foundation for Promotion of Cancer Research (K.O.), and the Japan–France Integrated Action Program (K.O. and C.G.).

References

1 Braithwaite AW, Prives CL. p53: more research and more questions. *Cell Death Differ* 2006; **13**: 877–80.
2 Levine AJ. p53, the cellular gatekeeper for growth and division. *Cell* 1997; **88**: 323–31.
3 Oren M. Decision making by p53: life, death and cancer. *Cell Death Differ* 2003; **10**: 431–42.
4 Ko LJ, Prives C. p53: puzzle and paradigm. *Genes Dev* 1996; **10**: 1054–72.
5 Vogelstein B, Lane D, Levine AJ. Surfing the p53 network. *Nature* 2000; **408**: 307–10.
6 Toledo F, Wahl GM. MDM2 and MDM4: p53 regulators as targets in anticancer therapy. *Int J Biochem Cell Biol* 2007; **39**: 1476–8.
7 Marine JC, Dyer MA, Jochemsen AG. MDMX: from bench to bedside. *J Cell Sci* 2007; **120**: 371–8.
8 Marine JC, Francoz S, Maetens M, Wahl G, Toledo F, Lozano G. Keeping p53 in check: essential and synergistic functions of Mdm2 and Mdm4. *Cell Death Differ* 2006; **13**: 927–34.
9 Linares LK, Hengstermann A, Ciechanover A, Muller S, Scheffner M. HdmX stimulates Hdm2-mediated ubiquitination and degradation of p53. *Proc Natl Acad Sci USA* 2003; **100**: 12 009–14.
10 Gu J, Kawai H, Nie L *et al.* Mutual dependence of MDM2 and MDMX in their functional inactivation of p53. *J Biol Chem* 2002; **277**: 19 251–4.
11 Tanimura S, Ohtsuka S, Mitsui K, Shirouzu K, Yoshimura A, Ohtsubo M. MDM2 interacts with MDMX through their RING finger domains. *FEBS Lett* 1999; **447**: 5–9.
12 Sharp DA, Kratowicz SA, Sank MJ, George DL. Stabilization of the MDM2 oncoprotein by interaction with the structurally related MDMX protein. *J Biol Chem* 1999; **274**: 38 189–96.
13 Michael D, Oren M. The p53–Mdm2 module and the ubiquitin system. *Semin Cancer Biol* 2003; **13**: 49–58.
14 Honda R, Tanaka H, Yasuda H. Oncoprotein MDM2 is a ubiquitin ligase E3 for tumor suppressor p53. *FEBS Lett* 1997; **420**: 25–7.
15 Coutts AS, La Thangue NB. Mdm2 widens its repertoire. *Cell Cycle* 2007; **6**: 827–9.
16 Stad R, Little NA, Xirodimas DP *et al.* Mdmx stabilizes p53 and Mdm2 via two distinct mechanisms. *EMBO Rep* 2001; **2**: 1029–34.
17 Toledo F, Krummel KA, Lee CJ *et al.* A mouse p53 mutant lacking the proline-rich domain rescues Mdm4 deficiency and provides insight into the Mdm2-Mdm4-p53 regulatory network. *Cancer Cell* 2006; **9**: 273–85.
18 Poyurovsky MV, Priest C, Kentsis A *et al.* The Mdm2 RING domain C-terminus is required for supramolecular assembly and ubiquitin ligase activity. *EMBO J* 2007; **26**: 90–101.
19 Uldrijan S, Pannekoek WJ, Vousden KH. An essential function of the extreme C-terminus of MDM2 can be provided by MDMX. *EMBO J* 2007; **26**: 102–12.
20 Shinozaki T, Nota A, Taya Y, Okamoto K. Functional role of Mdm2 phosphorylation by ATR in attenuation of p53 nuclear export. *Oncogene* 2003; **22**: 8870–80.
21 Laurie NA, Donovan SL, Shih CS *et al.* Inactivation of the p53 pathway in retinoblastoma. *Nature* 2006; **444**: 61–6.
22 Pereg Y, Shkedy D, de Graaf P *et al.* Phosphorylation of Hdmx mediates its Hdm2- and ATM-dependent degradation in response to DNA damage. *Proc Natl Acad Sci USA* 2005; **102**: 5056–61.

doi: 10.1111/j.1349-7006.2009.01180.x

23 Okamoto K, Kashima K, Pereg Y *et al.* DNA damage-induced phosphorylation of MdmX at serine 367 activates p53 by targeting MdmX for Mdm2-dependent degradation. *Mol Cell Biol* 2005; **25**: 9608–20.
24 Jin Y, Dai MS, Lu SZ *et al.* 14-3-3gamma binds to MDMX that is phosphorylated by UV-activated Chk1, resulting in p53 activation. *EMBO J* 2006; **25**: 1207–18.
25 Pereg Y, Lam S, Teunisse A *et al.* Differential roles of ATM- and Chk2-mediated phosphorylations of Hdmx in response to DNA damage. *Mol Cell Biol* 2006; **26**: 6819–31.
26 Chen L, Gilkes DM, Pan Y, Lane WS, Chen J. ATM and Chk2-dependent phosphorylation of MDMX contribute to p53 activation after DNA damage. *EMBO J* 2005; **24**: 3411–22.
27 Shmueli A, Oren M. Regulation of p53 by Mdm2: fate is in the numbers. *Mol Cell* 2004; **13**: 4–5.
28 Lopez-Pajares V, Kim MM, Yuan ZM. Phosphorylation of MDMX mediated by Akt leads to stabilization and induces 14-3-3 binding. *J Biol Chem* 2008; **283**: 13707–13.
29 Gu J, Nie L, Wiederschain D, Yuan ZM. Identification of p53 sequence elements that are required for MDM2-mediated nuclear export. *Mol Cell Biol* 2001; **21**: 8533–46.
30 Lohrum MA, Woods DB, Ludwig RL, Balint E, Vousden KH. C-terminal ubiquitination of p53 contributes to nuclear export. *Mol Cell Biol* 2001; **21**: 8521–32.
31 Xirodimas DP, Saville MK, Bourdon JC, Hay RT, Lane DP. Mdm2-mediated NEDD8 conjugation of p53 inhibits its transcriptional activity. *Cell* 2004; **118**: 83–97.
32 Toledo F, Wahl GM. Regulating the p53 pathway: *in vitro* hypotheses, *in vivo* veritas. *Nat Rev Cancer* 2006; **6**: 909–23.
33 Singh RK, Iyappan S, Scheffner M. Hetero-oligomerization with MdmX rescues the ubiquitin/Nedd8 ligase activity of RING finger mutants of Mdm2. *J Biol Chem* 2007; **282**: 10 901–7.
34 Becker K, Marchenko ND, Maurice M, Moll UM. Hyperubiquitylation of wild-type p53 contributes to cytoplasmic sequestration in neuroblastoma. *Cell Death Differ* 2007; **14**: 1350–60.
35 Moll UM, LaQuaglia M, Benard J, Riou G. Wild-type p53 protein undergoes cytoplasmic sequestration in undifferentiated neuroblastomas but not in differentiated tumors. *Proc Natl Acad Sci USA* 1995; **92**: 4407–11.
36 Lu W, Pochampally R, Chen L, Traidej M, Wang Y, Chen J. Nuclear exclusion of p53 in a subset of tumors requires MDM2 function. *Oncogene* 2000; **19**: 232–40.
37 Rodriguez-Lopez AM, Xenaki D, Eden TO, Hickman JA, Chresta CM. MDM2 mediated nuclear exclusion of p53 attenuates etoposide-induced apoptosis in neuroblastoma cells. *Mol Pharmacol* 2001; **59**: 135–43.
38 Danovi D, Meulmeester E, Pasini D *et al.* Amplification of Mdmx (or Mdm4) directly contributes to tumor formation by inhibiting p53 tumor suppressor activity. *Mol Cell Biol* 2004; **24**: 5835–43.
39 Jimenez GS, Khan SH, Stommel JM, Wahl GM. p53 regulation by post-translational modification and nuclear retention in response to diverse stresses. *Oncogene* 1999; **18**: 7656–65.
40 Li M, Brooks CL, Wu-Baer F, Chen D, Baer R, Gu W. Mono-versus polyubiquitination: differential control of p53 fate by Mdm2. *Science* 2003; **302**: 1972–5.
41 Li M, Brooks CL, Kon N, Gu W. A dynamic role of HAUSP in the p53–Mdm2 pathway. *Mol Cell* 2004; **13**: 879–86.
42 Meulmeester E, Maurice MM, Boutell C *et al.* Loss of HAUSP-mediated deubiquitination contributes to DNA damage-induced destabilization of Hdmx and Hdm2. *Mol Cell* 2005; **18**: 565–76.

Supporting Information

Additional Supporting Information may be found in the online version of this article:

Supporting Information Materials and Methods

Fig. S1. Non-phosphorylatable Mdmx cooperates with Mdm2 to suppress p53.

Fig. S2. Non-phosphorylatable Mdmx cooperates with Mdm2 to induce cytoplasmic localization of p53 in H1299.

Fig. S3. The Mdmx-3A mutation stimulates the localization of Mdm2 and p53 predominantly to the cytoplasm.

Fig. S4. Mdmx is required for cytoplasmic retention of p53 in neuroblastoma cells.

Please note: Wiley-Blackwell are not responsible for the content or functionality of any supporting materials supplied by the authors. Any queries (other than missing material) should be directed to the corresponding author for the article.

Ann Surg Oncol (2010) 17:967–972
DOI 10.1245/s10434-009-0865-y

Annals of
SURGICAL ONCOLOGY
OFFICIAL JOURNAL OF THE SOCIETY OF SURGICAL ONCOLOGY

ORIGINAL ARTICLE – COLORECTAL CANCER

TGM2 Is a Novel Marker for Prognosis and Therapeutic Target in Colorectal Cancer

Norikatsu Miyoshi, MD[1], Hideshi Ishii, MD[1,2], Koshi Mimori, MD[2], Fumiaki Tanaka, MD[2], Toshiki Hitora, MD[1], Mitsuyoshi Tei, MD[1], Mitsugu Sekimoto, MD[1], Yuichiro Doki, MD, PhD[1], and Masaki Mori, MD, PhD, FACS[1]

[1]Department of Gastroenterological Surgery, Osaka University Graduate School of Medicine, Osaka, Japan; [2]Division of Molecular and Surgical Oncology, Department of Molecular and Cellular Biology, Medical Institute of Bioregulation, Kyushu University, Ohita, Japan

ABSTRACT

Background. Transglutaminase 2 (*TGM2*) plays a role in cell growth and survival through the antiapoptosis signaling pathway.

Methods. We analyzed *TGM2* gene expression in 91 paired cases of colorectal cancer (CRC) and noncancerous regions and seven CRC cell lines to demonstrate the importance of *TGM2* expression for the prediction of prognosis of CRC. *TGM2* expression was higher in CRC tissue than in corresponding normal tissue by real-time reverse transcriptase–polymerase chain reaction ($P = .015$).

Results. Patients in the high *TGM2* expression group showed a poorer overall survival rate than those in the low expression group ($P = .001$), indicating that the increase in *TGM2* expression was an independent prognostic factor. *TGM2* was also expressed in the seven CRC cell lines. The in vitro proliferation assay showed that *TGM2* expression is involved with tumor growth.

Conclusions. The present study suggests that *TGM2* is useful as a predictive marker for patient prognosis and may be a novel therapeutic target for CRC.

Cancer is a major public health problem in developed countries, while the incidence of colorectal cancer (CRC) has greatly increased in Japan in recent years as a result of lifestyle changes.[1] CRC is now one of the most important causes of death from neoplastic disease in Japan.[1] Therefore, identification of the genes responsible for the development and progression of CRC and understanding the clinical significance are critical for the diagnosis and adequate treatment of the disease.

Transglutaminase 2, *TGM2*, is a family of enzymes that catalyzes the formation of an amide bond between the γ-carboxamide groups of peptide-bound glutamine residues and the primary amino groups in various compounds.[2,3] Several studies have reported that that increased expression of *TGM2* indicates prolonged cell survival and the prevention of apoptosis.[4–9]

We analyzed *TGM2* in seven human gastrointestinal cancer cell lines and 91 paired cases of CRC and noncancerous regions to identify the importance of *TGM2* expression for prognosis and to suggest that it be a candidate novel marker for the prognosis with functional relevance in CRCs.

MATERIALS AND METHODS

Clinical Tissue Samples

From 1992 to 2002, 91 patients (62 men, 29 women) with CRC underwent surgery at the Medical Institute of Bioregulation at Kyusyu University. Primary CRC specimens and adjacent normal colorectal mucosa were obtained from patients after receiving informed consent in accordance with the institutional guidelines. Every patient was definitively identified with CRC on the basis of clinicopathological findings. Tissues were extracted immediately after surgical resections. The specimens were immediately fixed in formalin, processed through graded ethanol,

Electronic supplementary material The online version of this article (doi:10.1245/s10434-009-0865-y) contains supplementary material, which is available to authorized users.

First Received: 20 July 2009;
Published Online: 22 December 2009

M. Mori, MD, PhD, FACS
e-mail: mmori@gesurg.med.osaka-u.ac.jp

embedded in paraffin, and sectioned with hematoxylin and eosin stain and elastica van Gieson stain, and the degree of the histological differentiation, lymphatic invasion, and venous invasion was examined. All specimens were frozen in liquid nitrogen immediately after resection and stored at −80°C until RNA extractions were performed.

None of the patients received chemotherapy or radiotherapy before surgery. After the surgery, the patients were followed up with a blood examination that included the tumor markers carcinoembryonic antigen and cancer antigen, and imaging modalities such as abdominal ultrasound, computed tomography, and chest x-ray every 3 to 6 months. Clinicopathological factors were assessed according to the criteria of the tumor node metastasis classification of the International Union Against Cancer.[10]

Cell Lines and Culture

Seven cell lines derived from human CRC (Caco2, DLD-1, HCT116, HT-29, KM12SM, LoVo, and SW480) were obtained and maintained in Dulbecco modified Eagle medium containing 10% fetal bovine serum and antibiotics at 37°C in a 5% humidified CO_2 atmosphere. For the siRNA knockdown experiment, double-stranded RNA duplexes targeting human *TGM2* (5′-UAGGAUCCCAUCUUCAA ACUGCCCA-3′/5′-UGGGCAGUUUGAAGAUGGGAUC CUA-3′, 5′-AUCCCAUUGUAGCUGACGGUGCGGG-3′/ 5′-CCCGCACCGUGAGCUACAAUGGGAU-3′, and 5′-UG UAGUUGGUCACGACGCGGGUAGG-3′/5′-CCUACCCG CGUCGUGACCAACUACA-3′) were purchased (Stealth RNAi) from Invitrogen (Carlsbad, CA). Negative control siRNA (NC) was also purchased from Invitrogen. CRC cell lines were transfected with siRNA at a concentration of 20 μmol/L with lipofectamine (RNAiMAX, Invitrogen), incubated in glucose-free Opti-MEM (Invitrogen) for the time indicated, and analyzed by the proliferation assay. All siRNA duplexes were used together as a triple transfection. siRNA knockdowns were performed in seven CRC cell lines to evaluate proliferation under *TGM2* suppression. Each cell line with siRNA was compared with the negative control. The values are presented as mean ± standard deviation (SD) from independent experiments conducted in triplicate.

RNA Preparation and Quantitative Real-Time Reverse Transcriptase–Polymerase Chain Reaction

Total RNA was prepared by using a modified acid guanidium-phenol-chloroform procedure with DNase.[11] Reverse transcription was performed from 2.5 μg of total RNA as previously described.[12] A 143-bp *TGM2* fragment was amplified. Two human *TGM2* oligonucleotide primers for the polymerase chain reaction (PCR) reaction were designed as follows: 5′-ATAAGTTAGCGCCGCTCTCC-3′ (forward); 5′-CCAGCTCCAGATCACACCTC-3′ (reverse). The forward primer is located in exon 1 and the reverse primer in exon 2. The PCR assay with primers specific to the glyceraldehyde-3-phosphate dehydrogenase (*GAPDH*) gene was performed to evaluate expression. The *GAPDH* primers, 5′-TTGGTATCGTGGAAGGACTCA-3′ (forward) and 5′-TGTCATCATATTGGCAGGTT-3′ (reverse), produced a 270-bp amplicon. cDNA from the Human Reference Total RNA (Clontech, Palo Alto, CA) was studied concurrently as a positive control. Real-time monitoring of the PCRs was performed with the LightCycler FastStart DNA Master SYBR Green I kit (Roche Diagnostics, Tokyo, Japan) for cDNA amplification of *TGM2* and *GAPDH*. The amplification protocol consisted of 35 cycles of denaturation at 95°C for 10 seconds, annealing at 60°C for 10 seconds, and elongation at 72°C for 10 seconds. The products were then subjected to a temperature gradient from 55°C to 95°C at 0.1°C per second with continuous fluorescence monitoring to produce product melting curves. The expression ratio of mRNA copies in tumor and normal tissues was calculated and normalized against *GAPDH* mRNA expression.

Proliferation Assays

In CRC cell lines transfected with siRNA, 1×10^5 cells were seeded in 12-well dishes and cultured for 96 hours to determine proliferation. The cell growth rate was measured by counting cells with a CellTac kit (Nihon Koden, Tokyo, Japan).

Statistical Analysis

Continuous variable data were expressed as mean ± SD. The relationship between mRNA expression and clinicopathological factors were analyzed by the χ^2 test and Student's *t*-test. Kaplan-Meier survival curves were plotted and compared with the generalized log rank test. Univariate and multivariate analyses to identify prognostic factors for overall survival were performed by the Cox proportional hazard regression model. All tests were analyzed by JMP software (SAS Institute, Cary, NC). *P* values of $<.05$ were considered statistically significant.

RESULTS

TGM2 mRNA Expression in Clinical Tissue Specimens

Reverse transcriptase–polymerase chain reaction (RT-PCR) of 91 paired clinical samples showed that 65 (71.4%) of the 91 cases exhibited higher levels of *TGM2* mRNA in tumors than paired normal tissues (Fig. 1). The mean *TGM2* mRNA expression value in tumor tissues was

significantly higher than that for corresponding normal tissues ($P = .015$; Student's *t*-test).

TGM2 Expression and Clinicopathological Characteristics

The experimental samples were divided into two groups according to expression status for the clinicopathological evaluation. Patients with tumors that had more than the median *TGM2/GAPDH* expression (median .329) were assigned to the high expression group ($n = 46$); the others were assigned to the low expression group ($n = 45$, Table 1). The number of cases that were based on histological grade was 37, 47, 4, and 3 in the well, moderate, poor, and mucinous adenocarcinoma categories, respectively. *TGM2* expression was correlated with tumor type ($P = .002$), tumor invasion ($P < .001$), lymph node metastasis ($P = .041$), lymphatic invasion ($P = .010$), metastasis ($P = .040$), and International Union Against Cancer stage ($P < .001$).

Relationship Between TGM2 Expression and Prognosis

Postoperative overall survival rate was statistically significantly lower in patients with increased *TGM2* expression (Fig. 2). The median follow-up was 4.12 years. Table 2 provides the univariate and multivariate analyses of factors related to patient prognosis. Univariate analysis showed that histological grade ($P = .040$), tumor type ($P = .003$), tumor size ($P = .004$), tumor invasion

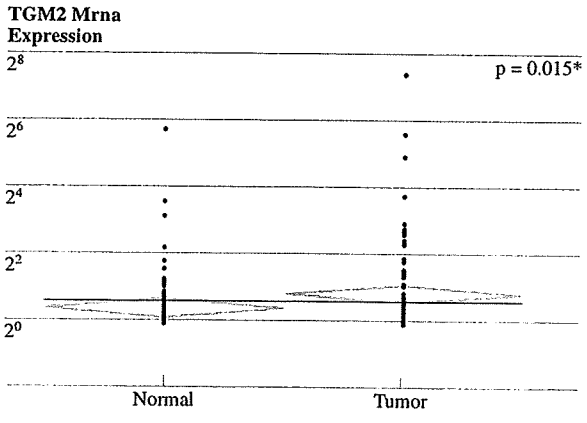

FIG. 1 Transglutaminase 2 (*TGM2*) mRNA expression in clinical tissue specimens. Quantitative real-time reverse transcriptase–polymerase chain reaction of 91 paired clinical samples showed that 65 (71.4%) of the 91 cases exhibited higher levels of *TGM2* mRNA in tumors than in paired normal tissues. The mean *TGM2* mRNA expression in tumor tissues (normalized by *GAPDH* gene expression) was significantly higher than that of the corresponding normal tissues ($P = .015$; Student's *t*-test)

TABLE 1 Clinicopathological factors and TGM2 mRNA expression in 91 colorectal cancers

Factor	High expression ($n = 46$)	Low expression ($n = 45$)	*P* value
Age (y)			
<68	25 (54.3%)	17 (37.8%)	.112
≥68	21 (45.7%)	28 (62.2%)	
Sex			
Male	31 (67.4%)	31 (68.9%)	.878
Female	15 (32.6%)	14 (31.1%)	
Histological grade			
Wel/Mod	41 (89.1%)	43 (95.6%)	.242
Others	5 (10.9%)	2 (4.4%)	
Tumor type			
0–2	0–2 3 (6.5%)	14 (31.1%)	.002*
3–4	3–4 43 (93.5%)	31 (68.9%)	
Tumor size			
<30 mm	39 (84.8%)	35 (77.8%)	.391
≥30 mm	7 (15.2%)	10 (22.2%)	
Tumor invasion			
Tis	0 (0%)	5 (11.1%)	≤.001*
T1	2 (4.3%)	6 (13.3%)	
T2	3 (6.5%)	12 (26.7%)	
T3	28 (60.9%)	18 (40.0%)	
T4	13 (28.3%)	4 (8.9%)	
Lymph node metastasis			
N0	22 (47.8%)	31 (68.9%)	.041*
N1–2	24 (52.2%)	14 (31.1%)	
Lymphatic invasion			
Absent	24 (52.2%)	35 (77.8%)	.010*
Present	22 (47.8%)	10 (22.2%)	
Venous invasion			
Absent	38 (82.6%)	40 (88.9%)	.392
Present	8 (17.4%)	5 (11.1%)	
Metastasis			
M0	29 (63.0%)	37 (82.2%)	.040*
M1	17 (37.0%)	8 (17.8%)	
UICC stage			
0	0 (0%)	5 (11.1%)	≤.001*
I	5 (10.9%)	12 (26.7%)	
IIA	11 (23.9%)	11 (24.4%)	
IIB	2 (4.3%)	1 (2.2%)	
IIIA	0 (0%)	5 (11.1%)	
IIIB	8 (17.4%)	3 (6.7%)	
IIIC	3 (6.5%)	0 (0%)	
IV	17 (37.0%)	8 (17.8%)	

Wel well differentiated adenocarcinoma, *mod* moderately differentiated adenocarcinoma, *others* poorly differentiated adenocarcinoma and mucinous carcinoma, *UICC* International Union Against Cancer

* Statistically significant

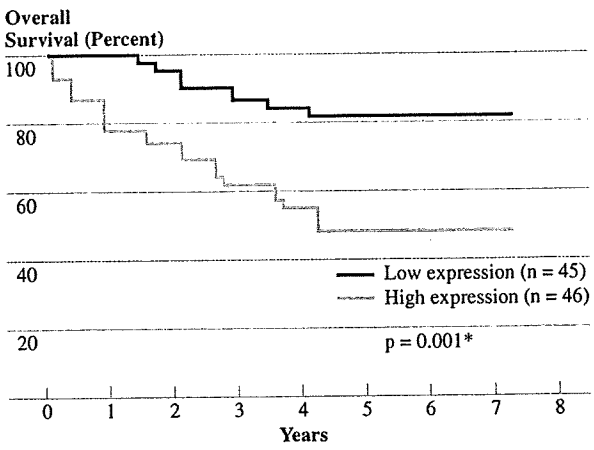

FIG. 2 Overall survival curves of colorectal cancer patients based on *TGM2* mRNA expression status. The postoperative overall survival rate was significantly lower among patients in the high *TGM2* expression group ($P = .001$, log rank test) than the low expression group. The median follow-up was 4.12 years

($P < .001$), lymph node metastasis ($P < .001$), lymphatic invasion ($P = .006$), venous invasion ($P = .001$), and *TGM2* mRNA expression ($P = .003$) were significantly related to overall survival. Multivariate analysis indicated that inclusion in the *TGM2* mRNA high expression group (relative risk, 2.40; 95% confidence interval, 1.03–6.11; $P = .041$) was an independent predictor of postoperative overall survival, as was metastasis (M1/M0, relative risk, 5.86; 95% confidence interval, 2.49–15.12; $P < .001$).

In Vitro Assessment of TGM2 Expression Knockdown

Seven CRC cell lines were used for the proliferation study because *TGM2* expression was higher than the median value of *GAPDH* in the primary CRC specimen by RT-PCR. A reduction in *TGM2* by siRNA was observed by quantitative real-time RT-PCR in all the cell lines examined (negative control [NC] and *TGM2* siRNAs; $P < .05$, Student's *t*-test). A reduction in *TGM2* expression was confirmed in the HT-29, HCT116, KM12SM, and LoVo cell lines (Suppl. Fig. S1). In proliferation assay, there were differences in cell numbers of HT-29 between NC and *TGM2* siRNA ($P < .05$) (Fig. 3). There was no statistically significant difference in the number between the NC and *TGM2* siRNA in the other cell lines.

DISCUSSION

Previous reports showed that *TGM2*, also known as *TG2*, is expressed in breast and pancreatic cancer cells and is associated with drug resistance and metastasis.[4–16] *TGM2* promotes a stable interaction with extracellular matrix protein components in association with some β members of the integrin family of proteins, which induce cell survival signaling pathways.[17] Other reports suggest that *TGM2* regulates activation of NF-κB by forming a ternary complex with NF-κB/IκBα, and inhibition of apoptosis through transamidation and GTP-binding activity.[4,9,18]

Seven distinct transglutaminases have been described.[19–22] *TGM2* is ubiquitously expressed as a single/polypeptide protein that exhibits Ca^{2+}-dependent protein cross-linking activity.[23]

We assessed *TGM2* gene expression and found that it was a statistically significant independent prognostic factor, similar to the well-known important predictive factor.[24] To our knowledge, the present study is the first report

TABLE 2 Univariate and multivariate analyses for overall survival (Cox proportional hazard regression model)

Factor	Univariate analysis			Multivariate analysis		
	RR	95% CI	*P* value	RR	95% CI	*P* value
Age (y), <68/≥68	1.47	0.70–3.11	.298			
Sex, male/female	1.40	0.64–3.38	.401			
Histological grade, por–others/well–mod	3.66	1.06–9.64	.040*	2.52	0.68–7.45	.148
Tumor type, 3–4/0–2	8.27	1.76–147.44	.003*	1.80	0.22–40.49	.615
Tumor size, ≥30 cm/<30 cm	2.82	1.30–11.91	.004*	1.26	0.45–6.02	.697
Tumor invasion, T3–4/Tis-2	7.60	2.27–47.16	≤.001*	1.13	0.36–2.68	.802
Lymph node metastasis, N1–2/N0	5.42	2.43–13.74	≤.001*	2.06	0.83–5.74	.119
Lymphatic invasion, present/absent	2.80	1.34–5.89	.006*	1.32	0.53–3.22	.532
Venous invasion, present/absent	4.20	1.81–9.03	.001*	2.24	0.85–5.80	.099
Metastasis, M1/M0	8.93	4.14–20.84	≤.001*	5.86	2.49–15.12	≤.001*
TGM2 mRNA expression, ≥median/median>	3.08	1.43–7.18	.003*	2.40	1.03–6.11	.041*

RR relative risk, *95% CI* 95% confidence interva, *wel* well-differentiated adenocarcinoma, *mod* moderately differentiated adenocarcinoma, *por* poorly differentiated adenocarcinoma, *others* poorly differentiated adenocarcinoma and mucinous carcinoma

* Statistically significant

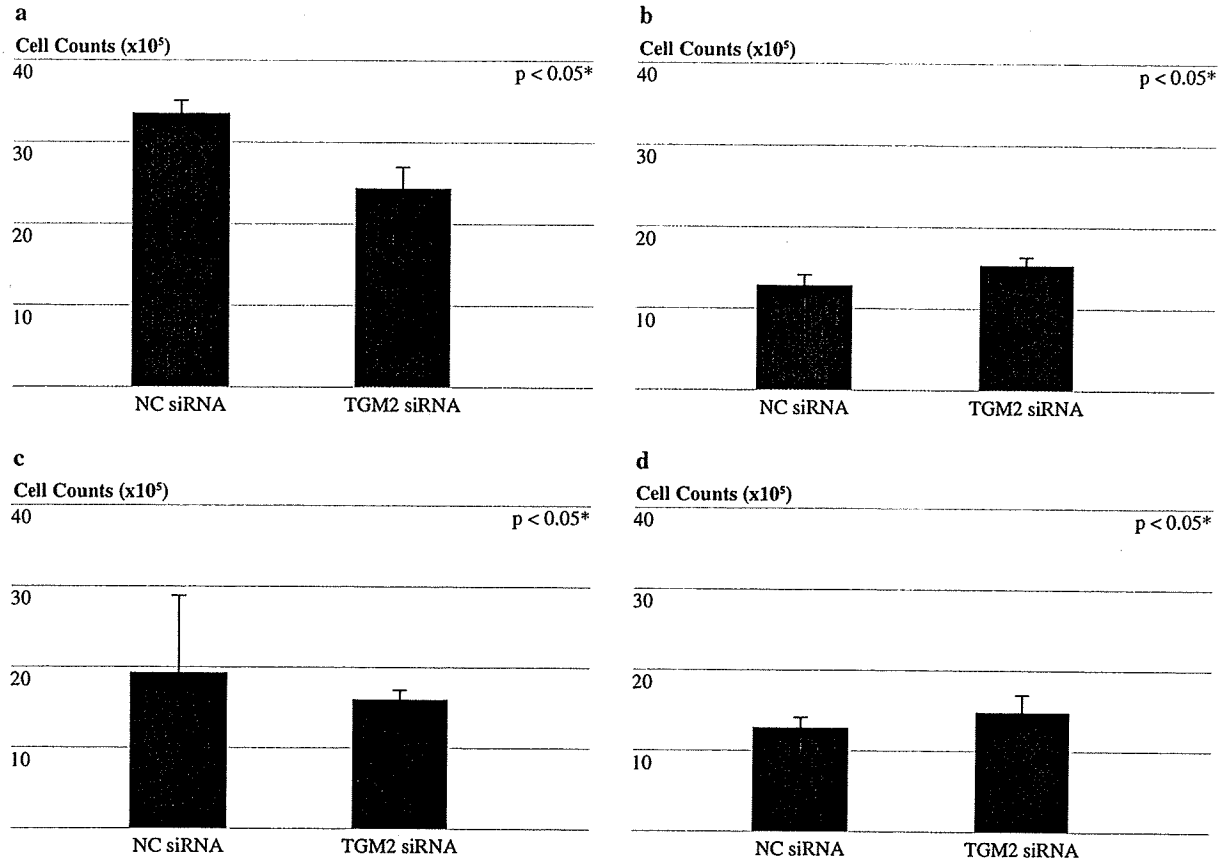

FIG. 3 Proliferation assay and siRNA inhibition in 4 colorectal cancer cell lines. The proliferation assay showed a difference in growth of colorectal cancer cell line HT-29. There were significant differences between NC and *TGM2* siRNA. In the other 3 cell lines, there was no significant difference between NC and *TGM2* siRNA (**a** HT-29; **b** HCT116; **c** KM12SM; **d** LoVo). Values are mean ± SD for three independent experiments. WT, wild type; NC, negative control

showing that *TGM2* is upregulated in CRCs, suggesting that it could be a novel predictive marker for the prognosis of CRCs that may contribute to further clinical cancer diagnosis.

Recently, the necessity of intensive follow-up and adjuvant therapy for CRC has been proposed to predict recurrence and metastasis in curative surgical resected cases.[25–27] In addition, there have been many recent reports on the use of less invasive surgery for CRC such as laparoscopic and endoscopic surgery.[28–31] For these cases, a predictive marker of tumor invasion, lymph node metastasis, and distant metastasis would play a very important role in cancer diagnoses and treatments, especially as a novel marker independent from the traditional tumor, node, metastasis factors. Thus, the *TGM2* expression profile could contribute to the predictive diagnosis of CRCs.

TGM2 plays an important role in antiapoptotic signaling pathways and several cancer cell lines that exhibit high *TGM2* expression levels and have been selected for resistance to chemotherapeutic drugs.[17,32,33] Downregulation of *TGM2* expression by siRNA rendered the cancer cells sensitive to chemotherapeutic drugs.[17]

The present in vitro study showed that *TGM2* expression is associated with tumor growth, and the inhibition of *TGM2* may lead to a reduction in CRC proliferation. *TGM2* is expressed in several cancers.[14–16] Our results suggest a rationale for further study of *TGM2* as a possible novel target for clinical cancer therapy such as anticancer agents and the sensitizer in addition to the novel marker of prognosis and prediction about the susceptibility of anticancer agents.

REFERENCES

1. Kohno SI, Luo C, Nawa A, et al. Oncolytic virotherapy with an HSV amplicon vector expressing granulocyte-macrophage colony-stimulating factor using the replication-competent HSV type 1 mutant HF10 as a helper virus. *Cancer Gene Ther.* 2007;14: 918–26.
2. Folk JE. Transglutaminases. *Annu Rev Biochem.* 1980;49: 517–31.

3. Lorand L, Graham RM. Transglutaminases: crosslinking enzymes with pleiotropic functions. *Nat Rev Mol Cell Biol.* 2003; 4:140–56.
4. Antonyak MA, Singh US, Lee DA, et al. Effects of tissue transglutaminase on retinoic acid–induced cellular differentiation and protection against apoptosis. *J Biol Chem.* 2001;276:33582–7.
5. Boehm JE, Singh U, Combs C, et al. Tissue transglutaminase protects against apoptosis by modifying the tumor suppressor protein p110 Rb. *J Biol Chem.* 2002;277:20127–30.
6. Antonyak MA, Miller AM, Jansen JM, et al. Augmentation of tissue transglutaminase expression and activation by epidermal growth factor inhibit doxorubicin-induced apoptosis in human breast cancer cells. *J Biol Chem.* 2004;279:41461–7.
7. Mangala LS, Mehta K. Tissue transglutaminase (TG2) in cancer biology. *Prog Exp Tumor Res.* 2005;38:125–38.
8. Mehta K. Mammalian transglutaminases: a family portrait. *Prog Exp Tumor Res.* 2005;38:1–18.
9. Mann AP, Verma A, Sethi G, et al. Overexpression of tissue transglutaminase leads to constitutive activation of nuclear factor-kappaB in cancer cells: delineation of a novel pathway. *Cancer Res.* 2006;66:8788–95.
10. Sobin LH, Fleming ID. TNM classification of malignant tumors, 5th edn. Union Internationale Contre le Cancer and the American Joint Committee on Cancer. *Cancer.* 1997;80:1803–4.
11. Mimori K, Mori M, Shiraishi T, et al. Clinical significance of tissue inhibitor of metalloproteinase expression in gastric carcinoma. *Br J Cancer.* 1997;76:531–6.
12. Mori M, Staniunas RJ, Barnard GF, et al. The significance of carbonic anhydrase expression in human colorectal cancer. *Gastroenterology.* 1993;105:820–6.
13. Fesus L, Piacentini M. Transglutaminase 2: an enigmatic enzyme with diverse functions. *Trends Biochem Sci.* 2002;27:534–9.
14. Mehta K. High levels of transglutaminase expression in doxorubicin-resistant human breast carcinoma cells. *Int J Cancer.* 1994;58:400–6.
15. Chen JS, Konopleva M, Andreeff M, et al. Drug-resistant breast carcinoma (MCF-7) cells are paradoxically sensitive to apoptosis. *J Cell Physiol.* 2004;200:223–34.
16. Mehta K, Fok J, Miller FR, et al. Prognostic significance of tissue transglutaminase in drug resistant and metastatic breast cancer. *Clin Cancer Res.* 2004;10:8068–76.
17. Herman JF, Mangala LS, Mehta K. Implications of increased tissue transglutaminase (TG2) expression in drug-resistant breast cancer (MCF-7) cells. *Oncogene.* 2006;25:3049–58.
18. Sarang Z, Molnar P, Nemeth T, et al. Tissue transglutaminase (TG2) acting as G protein protects hepatocytes against Fas-mediated cell death in mice. *Hepatology.* 2005;42:578–87.
19. Aeschlimann D, Paulsson M. Transglutaminases: protein cross-linking enzymes in tissues and body fluids. *Thromb Haemost.* 1994;71:402–15.
20. Aeschlimann D, Koeller MK, Allen-Hoffmann BL, Mosher DF. Isolation of a cDNA encoding a novel member of the transglutaminase gene family from human keratinocytes. Detection and identification of transglutaminase gene products based on reverse transcription–polymerase chain reaction with degenerate primers. *J Biol Chem.* 1998;273:3452–60.
21. Chen JS, Mehta K. Tissue transglutaminase: an enzyme with a split personality. *Int J Biochem Cell Biol.* 1999;31:817–36.
22. Greenberg CS, Birckbichler PJ, Rice RH. Transglutaminases: multifunctional cross-linking enzymes that stabilize tissues. *FASEB J.* 1991;5:3071–7.
23. Ai L, Kim WJ, Demircan B, et al. The transglutaminase 2 gene (*TGM2.*), a potential molecular marker for chemotherapeutic drug sensitivity, is epigenetically silenced in breast cancer. *Carcinogenesis.* 2008;29:510–8.
24. Andre T, Quinaux E, Louvet C, et al. Phase III study comparing a semimonthly with a monthly regimen of fluorouracil and leucovorin as adjuvant treatment for stage II and III colon cancer patients: final results of GERCOR C96.1. *J Clin Oncol.* 2007;25: 3732–8.
25. Wolpin BM, Mayer RJ. Systemic treatment of colorectal cancer. *Gastroenterology.* 2008;134:1296–10.
26. Kornmann M, Formentini A, Ette C, et al. Prognostic factors influencing the survival of patients with colon cancer receiving adjuvant 5-FU treatment. *Eur J Surg Oncol.* 2008;34:1316–21.
27. Bathe OF, Dowden S, Sutherland F, et al. 2004 Phase II study of neoadjuvant 5-FU + leucovorin + CPT-11 in patients with resectable liver metastases from colorectal adenocarcinoma. *BMC Cancer.* 4:32.
28. Lacy AM, Garcia-Valdecasas JC, Delgado S, et al. Laparoscopy-assisted colectomy versus open colectomy for treatment of non-metastatic colon cancer: a randomised trial. *Lancet.* 2002;359: 2224–9.
29. Weeks JC, Nelson H, Gelber S, et al. Short-term quality-of-life outcomes following laparoscopic-assisted colectomy vs open colectomy for colon cancer: a randomized trial. *JAMA.* 2002;287: 321–8.
30. Group COoSTS. 2004 A comparison of laparoscopically assisted and open colectomy for colon cancer. *N Engl J Med.* 350:2050–9.
31. Jayne DG, Guillou PJ, Thorpe H, et al. Randomized trial of laparoscopic-assisted resection of colorectal carcinoma: 3-year results of the UK MRC CLASICC Trial Group. *J Clin Oncol.* 2007;25:3061–8.
32. Han JA, Park SC. Reduction of transglutaminase 2 expression is associated with an induction of drug sensitivity in the PC-14 human lung cancer cell line. *J Cancer Res Clin Oncol.* 1999;125: 89–95.
33. Devarajan E, Chen J, Multani AS, et al. Human breast cancer MCF-7 cell line contains inherently drug-resistant subclones with distinct genotypic and phenotypic features. *Int J Oncol.* 2002;20:913–20.